Developmental Biology 346 (2010) 39–53

Contents lists available at ScienceDirect

Developmental Biology

journal homepage: www.elsevier.com/developmentalbiology

The ATP-sensitive K^+-channel (K_{ATP}) controls early left–right patterning in *Xenopus* and chick embryos

Sherry Aw [a,b,1], Joseph C. Koster [c], Wade Pearson [c], Colin G. Nichols [c], Nian-Qing Shi [d], Katia Carneiro [a], Michael Levin [a,*]

[a] Center for Regenerative and Developmental Biology, and Biology Department, Tufts University, Medford, MA 02155, USA
[b] Program in Biological and Biomedical Sciences, Harvard Medical School, Boston, Massachusetts 02115, USA
[c] Department of Cell Biology and Physiology, and Center for the Investigation of Membrane Excitability Diseases, Washington University School of Medicine, St. Louis, MO 63110, USA
[d] Department of Medicine, University of Wisconsin, Madison, WI 53706, USA

ARTICLE INFO

Article history:
Received for publication 30 April 2010
Revised 21 June 2010
Accepted 8 July 2010
Available online 17 July 2010

Keywords:
Left–right asymmetry
K_{ATP} channels
Kir6.1
Tight junctions
Xenopus

ABSTRACT

Consistent left–right asymmetry requires specific ion currents. We characterize a novel laterality determinant in *Xenopus laevis*: the ATP-sensitive K^+-channel (K_{ATP}). Expression of specific dominant-negative mutants of the *Xenopus* Kir6.1 pore subunit of the K_{ATP} channel induced randomization of asymmetric organ positioning. Spatio-temporally controlled loss-of-function experiments revealed that the K_{ATP} channel functions asymmetrically in LR patterning during very early cleavage stages, and also symmetrically during the early blastula stages, a period when heretofore largely unknown events transmit LR patterning cues. Blocking K_{ATP} channel activity randomizes the expression of the left-sided transcription of *Nodal*. Immunofluorescence analysis revealed that *X*Kir6.1 is localized to basal membranes on the blastocoel roof and cell–cell junctions. A tight junction integrity assay showed that K_{ATP} channels are required for proper tight junction function in early *Xenopus* embryos. We also present evidence that this function may be conserved to the chick, as inhibition of K_{ATP} in the primitive streak of chick embryos randomizes the expression of the left-sided gene *Sonic hedgehog*. We propose a model by which K_{ATP} channels control LR patterning via regulation of tight junctions.

Introduction

The large-scale body plan of an organism strongly determines major aspects of its physiology and behavior. Most vertebrates exhibit an external bilateral symmetry that belies a consistently biased internal left–right (LR) asymmetry, and perturbations in normal LR patterning result in defects that can be medically significant (Peeters and Devriendt, 2006; Ramsdell, 2005).

Studies over the last 15 years have begun to reveal the pathways determining laterality in embryonic development (Aw and Levin, 2008; Basu and Brueckner, 2008; Speder et al., 2007; Vandenberg and Levin, 2009). Consistent alignment of internal organs requires an initial chiral element to be oriented with respect to the anterior–posterior and dorso-ventral axes. This information is then transmitted and amplified to the developing organs that undergo asymmetric morphogenesis (Brown and Wolpert, 1990; Levin, 2006). In vertebrates, the downstream steps involve activation of molecules from *hedgehog*, FGF, EGF-CFC, BMP, and other families (Burdine and Schier, 2000; Levin, 1998), which induce a conserved (Yost, 1999; Yost, 2001) left-specific Nodal signaling (Whitman and Mercola, 2001a; Yost, 2001) gene cascade from the node to the left lateral plate mesoderm (Whitman and Mercola, 2001b). However, the symmetry-breaking steps upstream of asymmetric gene expression are more controversial (Levin and Palmer, 2007; Tabin, 2005).

One model proposes that net unidirectional extracellular fluid flow established by cilia at the node organizer during late gastrulation sets up gradients of morphogens that drive asymmetric gene expression (Basu and Brueckner, 2008; Tabin and Vogan, 2003). On this proposal, the chiral centriole/microtubule-organizing center (MTOC) is amplified into multicellular LR asymmetry by establishing the direction of ciliary motion with respect to the other two axes.

A different model (Levin and Nascone, 1997; Levin and Palmer, 2007) focuses on the role of the centriole/MTOC in biasing intracellular cytoskeletal organization (Danilchik et al., 2006; Qiu et al., 2005; Xu et al., 2007). The chiral cytoskeleton allows molecular motors (kinesin and dynein) to localize specific cargo to the left and right blastomeres. This includes ion channels and pumps whose asymmetric localization sets up differential voltage gradients on the left and right sides. This, in turn, establishes asymmetric gene expression (Aw and Levin, 2009; Levin, 2006). Work in chick, frog,

* Corresponding author. 200 Boston Ave. Suite 4600, Medford, MA 02155, USA. Fax: +1 617 627 6121.
E-mail address: michael.levin@tufts.edu (M. Levin).
[1] Current Address: Department of Neuroscience and Behavioural Disorders, Duke-NUS Graduate Medical School, Singapore.

0012-1606/$ – see front matter © 2010 Elsevier Inc. All rights reserved.
doi:10.1016/j.ydbio.2010.07.011

sea-urchin, zebrafish, and *Ciona* have implicated several ion transporters in left–right asymmetry (Adams et al., 2006a; Duboc et al., 2005; Hibino et al., 2006; Levin et al., 2002; Raya et al., 2004; Shimeld and Levin, 2006).

In *Xenopus*, recent work identified the V-ATPase H^+ pump (Adams et al., 2006b), H^+/K^+-ATPase exchanger (Levin et al., 2002), and the KCNQ1 and Kir4.1 potassium channels (Aw et al., 2008b; Morokuma et al., 2008) as required for LR patterning upstream of left-sided Nodal expression. The resulting endogenous asymmetric changes in ion flux and transmembrane potential operate during early cleavage stages (Adams et al., 2006b; Levin et al., 2002).

Here, we describe the identification of a new player in LR patterning, the ATP-sensitive K^+-channel channel (K_{ATP}). K_{ATP} channels belong to the family of inwardly rectifying potassium (K_{ir}) channels (Kubo et al., 2005; Nichols, 2006; Noma, 1983; Reimann and Ashcroft, 1999). They are gated by the ratio of ATP:MgADP in the cell, and hence couple the metabolic state of the cell to its membrane potential. When the ATP:MgADP ratio is elevated, K_{ATP} channels close causing membrane depolarization, and Ca^{2+}-entry through voltage sensitive Ca^{2+}-channels. Conversely, when the nucleotide ratio is decreased, K_{ATP} channels open, resulting in membrane hyperpolarization and cessation of Ca^{2+}-entry. K_{ATP} channels are comprised of four pore-forming Kir6.x subunits (either Kir6.1 or Kir6.2), surrounded by four regulatory sulphonylurea receptor subunits (SUR1 or SUR2), which are members of the ATP-binding cassette (ABC) transporter superfamily. K_{ATP} channels are found in many tissue types, including the pancreatic β-cell (Ashcroft et al., 1984; Findlay et al., 1985), brain (Ashford et al., 1988), and striated and smooth muscle (Spruce et al., 1985; Standen et al., 1989), with different tissues expressing K_{ATP} channels with differing physiological properties. The critical roles that K_{ATP} channels play have been highlighted by K_{ATP} mutations that underlie several important human diseases, including hyperinsulinism, diabetes (Masia et al., 2007; Shimomura, 2009; Sivaprasadarao et al., 2007), heart disease (Bienengraeber et al., 2004; Kane et al., 2005; Miki and Seino, 2005), and hypertension (Chutkow et al., 2002; Kane et al., 2006).

We carried out loss-of-function experiments in *Xenopus* which demonstrate that K_{ATP} is necessary for normal embryonic asymmetry. K_{ATP} was required in LR patterning during very early cleavage and also during blastula stages, a developmental period during which very little is known with respect to the LR pathway. We provide evidence that K_{ATP} may regulate tight junctions, which are known to be important for correct LR patterning (Brizuela et al., 2001; Simard et al., 2006; Vanhoven et al., 2006). We present functional data that show that this function may be conserved to the chick. Our findings identify a novel role for the K_{ATP} channel, and reveal a new molecular component functioning in the time period between early physiological asymmetries (Fukumoto et al., 2005; Levin et al., 2006) and subsequent ciliary flows during neurulation (Schweickert et al., 2007).

Materials and methods

Animal husbandry

Xenopus embryos were collected according to standard protocols (Sive et al., 2000) in 0.1× Modified Marc's Ringers (MMR) pH 7.8 + 0.1% Gentamicin and staged according to (Nieuwkoop and Faber, 1967).

Laterality assays

Xenopus embryos at st. 46 were analyzed for position (*situs*) of 3 organs: the heart, stomach, and gallbladder (Levin and Mercola, 1998a). Heterotaxia was defined as reversal in position of one or more organs. Only embryos with normal dorso-anterior development (DAI = 5) were scored in order to avoid scoring instances of secondary randomization due to errors in the DV or AP axial patterning (Danos and Yost, 1996), and only clear left- or right-sided organs were scored. Percent heterotaxia was calculated as number with heterotaxia divided by the number of total scorable embryos, i.e. embryos normal in all other ways, with DAI = 5. A χ^2 test (with Pearson correction for increased stringency) was used to compare absolute counts of heterotaxic embryos.

Molecular biology

Degenerate PCR of K_{ATP} subunits was carried out using standard PCR procedures using Takara Bioscience's KOD HotStart DNA Polymerase. cDNA libraries for RACE PCR were generated from RNAs from stage 10.5, 15 and 25 embryos using Clontech's sMART RACE kit. DNxKir6.1-pore construct was created using standard mutagenesis PCR procedures to mutate the pore-loop GFG to AAA. This motif has critical roles in selectivity and pore function (Doyle et al., 1998; Heginbotham et al., 1994; Jiang et al., 2003; Slesinger et al., 1996). DNxKir6.1-ER construct was created by fusing the endoplasmic reticulum (ER)-retention motif KHILFRRRRRGFRQ to the C terminus of xKir6.1 (Schwappach et al., 2000). Because channel assembly occurs in the ER, this dominant-negative (DN) construct is expected to assemble with and trap wild-type (WT) subunits in the ER, hence inhibiting their function at the plasma membrane (Ficker et al., 2000). Dominant-negatives against Kir2.1 and Kir2.2 were gifts of Peter Backx (Zobel et al., 2003). DNKir2.3 was a gift of D. Wray (Bannister et al., 1999).

Xenopus microinjection

For microinjections, capped, synthetic mRNAs (Sive et al., 2000), generated using the Ambion mMessage mMachine kit were dissolved in water and injected into embryos in 3% Ficoll using standard methods (100 ms pulses in each injected cell with borosilicate glass needles calibrated for a bubble pressure of 50–60 kPa in water). Each injection delivered between 1 and 3 nL or 0.5 and 3 ng of mRNA into the embryo, usually into the middle of the cell in the animal pole, except for the left–right sorting experiments at one cell, in which injections were made off center. 30 min post-injection, embryos were washed into 0.5× MMR for 30 min, and then cultured in 0.1× MMR until desired stages.

Drug exposure

Our pharmacological screen has been previously described (Adams et al., 2006a; Levin et al., 2002). *Xenopus* embryos were incubated in pharmacological blockers or openers during the stages of interest depending on the experiment (for the initial drug screen, embryos were incubated from Stage 1 cell to Stage 16, typical doses listed in Supplemental Table 1), and then transferred to 0.1× MMR and scored for organ reversals at stage 46. Drug dosages were titered to ensure that the dorso-anterior index of the treated embryos was normal (DAI = 5). K_{ATP} channel blocker HMR-1098 was a gift from H. Gogelein (Dhein et al., 2000; Edwards et al., 2009; Gogelein et al., 2001; Kaab et al., 2003; Light et al., 2001; Suzuki et al., 2003) and used at 1.45 mM. In the chick experiments, chick embryos were incubated in the respective drugs from the beginning of incubation to Stage 4^+ before being processed for *in situ* hybridization. Repaglinide was used at a final concentration of 10.6 μM and diazoxide was used at 200 μM.

Immunohistochemistry

Xenopus embryos were fixed for 2 h at room temperature in MEMFA, transferred to ethanol through a 25%/50%/75% series, and then stored at −20 °C in 100% ethanol. When ready to be sectioned, they were rehydrated, cleared for 2×15 min in Citrisolv (Fisherbrand), washed once with 50%/50% Citrisolv/paraffin, incubated in 4 changes of paraffin for 30 min each, and then embedded in paraffin. 5 μm thick sections through paraffin-embedded embryos were made on a manual steel microtome. Sections were mounted

onto VWR Superfrost Plus slides by floating on a warm water bath, then dewaxed with Citrisolv and rehydrated.

For immunohistochemical studies, antigens were unmasked by boiling sections in 0.01 M sodium citrate (pH 6.0) for 4 min at 60% power in a microwave in plastic coupling jars. Slides were cooled in coupling jars for 30 min on the bench top, then washed 3×3 min in 1× PBS, blocked in 5% goat serum in 1× PBS for 1 h at room temperature, then incubated with the appropriate dilution of primary antibody in blocking solution for 1 h at room temperature. Primary antibodies anti-Kir6.1 (Alomone Labs), and anti-SUR2 (Pu et al., 2008) were diluted at 1:250, 1:250. Slides were then washed twice for 3 min in 1× PBS, and incubated with Alexa 647 secondary antibody (Molecular Probes) at 1:200 dilution in 1× PBS for 1 h at room temperature in a humidified chamber. Slides were then washed twice for 3 min in 1× PBS and mounted using VectorShield Media with a coverslip and analyzed.

Western blotting

Thirty *Xenopus* embryos were resuspended in 520 µl lysis buffer (1% Triton X100, 50 mM NaCl, 10 mM NaF, 1 mM Na3VO4, 5 mM EDTA, 10 mM Tris pH 7.6, 2 mM PMSF). Protein solution was mixed at 1:1 with Laemmli sample buffer (Biorad) containing 2.5% 2-mercaptoethanol. The proteins were fractionated by SDS-PAGE and electrotransferred to a PVDF membrane. After washing, the membrane was blocked with 5% dry milk in 1× PBS with 0.1% Tween-20 (PBST) and then incubated overnight in a Mini-PROTEAN II multiscreen apparatus (Biorad) at 4 °C with the primary antibody, diluted in 5% dry milk in PBST (1:2000 for anti-Kir6.1 (Alomone Labs), 1:1000 for anti-SUR2, 1:1000 for anti-c-myc (Sigma)). After washing, the blots were incubated with peroxidase-conjugated second antibody (1:20,000) and developed using Pierce SuperSignal West Pico Chemiluminescent substrate according to the manufacturer's instructions.

Chromogenic in situ hybridization

In situ hybridization was performed as previously described (Harland, 1991). *Xenopus* embryos were collected and fixed in MEMFA for 2 h at room temperature (23 °C), washed in PBS + 0.1% Tween-20 and then transferred to ethanol through a 25%/50%/75% series and stored at −20 °C until ready to be processed. Probes for in situ hybridization were generated in vitro from linearized templates using DIG labeling mix from Invitrogen. Chromogenic reaction times were optimized for signal to background ratio.

Detection of K_{ATP} channel activity

Measurements of membrane potential in *Xenopus* laevis embryos were made using sharp electrode impalements in a small (600 µl) Plexiglass recording chamber mounted on the stage of a binocular microscope (SMZ-1, Nikon Instruments). The chamber was constantly perfused by a laminar gravity flow through multiple inlet lines allowing rapid solution changes, connected to a manifold at the inlet to the chamber. The chamber was also connected through Ag/AgCl electrodes in 1% agar bridges to the current-sensing headstage of a voltage clamp amplifier (OC-725C Oocyte Clamp, Warner Instruments) controlled by pCLAMP software (Axon Instruments, Foster City, CA, USA). The exchange rate for the external solution surrounding the embryo was about 95% in less than a minute. Experiments were performed at room temperature (23 °C). Intracellular recording electrodes were pulled from thin-walled borosilicate glass (TW-150-F4, WPI, Sarasota, FL, USA), filled with 3 M KCl, and had initial resistance of 0.3–1.0 MΩ. Data were digitized on-line and stored on a computer, or were digitized at 2 kHz onto videotape (Neuro-corder DR-890, Neuro-Data Instruments) for off-line analysis. Membrane potentials were recorded in 0.1× MMR, with addition of azide, 250 µM diazoxide (Sigma) or 5 µM glibenclamide as indicated (diazoxide and glibenclamide were dissolved as stock solution in DMSO, then diluted to <1% DMSO). A single embryo was simultaneously impaled with two electrodes in separate regions during a typical experiment.

Rubidium efflux assay for K_{ATP} channel activity

COSm6 cells were plated at a density of approximately 2.5×105 cells per well in 30 mm 6-well tissue culture dishes and cultured in Dulbecco's modified Eagle's medium plus 10 mM glucose (DMEM-HG), supplemented with 10% fetal calf serum, penicillin (100 U/ml) and streptomycin (100 µg/ml). The next day, cells were transfected by incubation for 1 h at 37 °C in serum-free DMEM-HG medium containing 2% Fugene-6 transfection reagent (Roche Diagnostics, Indianapolis, IN USA), and 400 ng each of combinations of the following cDNAs as described for each experiment: pCDNA-xKir6.1, pCDNA-mKir6.2, pECE-SUR1, pCDNA-DNxKir6.1-pore and pCDNA-DNxKir6.1-ER. Cells were incubated in the presence of the transfection mixture for 12–24 h.

For the rubidium flux experiments, ^{86}RbCl (1 mCi/ml) was added in fresh growth medium, 48 h after transfection. Cells were incubated for an additional 24 h and then incubated for 10 min at 25 °C in Krebs–Ringer solution with metabolic inhibitors (2.5 µg/ml oligomycin plus 1 mM 2-deoxy-D-glucose). At selected time points, solution was aspirated from the media for counting of $^{86}Rb^{+}$ in a scintillation counter, and replaced with fresh solution.

Biotin-labeling assay for tight junction permeability

We used a biotin-labeling assay (as described in Merzdorf et al., 1998) to probe tight junction permeability of embryos. Sulfo-NHS-LC-Biotin (Pierce) is a modified biotin with long 22.4 Å spacer arms making the molecule too large to bypass tight junctions. It contains a highly charged sulfo-group, which prevents it from entering the cell membrane. The biotin group allows it to covalently label primary amines like lysine side chains and N-terminal alpha amines. Hence, only exposed amines on the surface of the embryo will be labeled, and not membranes of inner blastomeres, unless cell–cell tight junction barriers are broken. Just before Stage 7, embryos were placed in 0.1× MMR cooled to 10 °C. Embryos were then transferred to fresh 1 mg/ml EZ-Link Sulfo-NHS-LC-Biotin (Pierce) in 0.1× MMR with 10 mM HEPES (pH 7.8), and labeled at 10 °C for 12 min. After labeling, embryos were rinsed twice with cooled 0.1× MMR and fixed in 5% paraformaldehyde made fresh from paraformaldehyde in 80 mM sodium cacodylate, at room temperature for 1 h, then dehydrated in ethanol and stored before sectioning and processed for immunohistochemistry with streptavidin-Alexa 555 (Molecular Probes).

Chick whole-mount in situ hybridization

In situ hybridization was performed as previously described (Nieto et al., 1996). *Sonic hedgehog* probe was as described in Levin et al. (1995); cKir6.1 probe was as described in Lu and Halvorsen (1997).

Image acquisition

Immunofluorescence samples were mounted onto glass slides for viewing, and were imaged using the Semrock CY5-4040A (Ex 628/40-Di 660/18, Em 692/40) cube set on an Olympus BX61 microscope with an ORCA AG digital CCD camera (Hamamatsu) with IPLabs software at approximately 23 °C. Lenses used were: 4× U Plan S-Apo NA = 0.16, 10× U Plan S-Apo NA = 0.4, 20× U Plan S-Apo NA = 0.70, 40× U Plan S-Apo NA = 0.90, and 60× Plan Apo Oil NA = 1.45.

Results

K_{ATP} channel function is necessary for correct LR patterning

To identify ion-dependent signals in left–right (LR) patterning, we carried out a hierarchical pharmacological screen (Adams and Levin, 2006a,b). Embryos were incubated in different blockers of ion channels and pumps and then scored for the sidedness of the heart, stomach and gall bladder at Stage 46 (Figs. 1A–E). Only embryos with no other observable abnormalities were scored, in order to rule out secondary effects from toxicity. Embryos in which any of these three organs was reversed were scored as "heterotaxic". We found that potassium channel blockers, but not sodium, chloride or calcium channel blockers, caused statistically significant rates of heterotaxia. Using inhibitors that distinguish among various families of potassium channels, we then found that 6 blockers of K_{ATP} caused heterotaxia (Supplement 1 and Supplemental Table 1).

We cloned *Xenopus laevis* K_{ATP} subunit xKir6.1 (Supplement 2) by degenerate PCR. The amino acid sequence of xKir6.1 is highly similar to human and mouse Kir6.1 (93% similar), and related to human/mouse Kir6.2 (84% similar, alignment not shown). To inhibit K_{ATP} activity with molecular specificity, we introduced mRNAs coding for dominant-

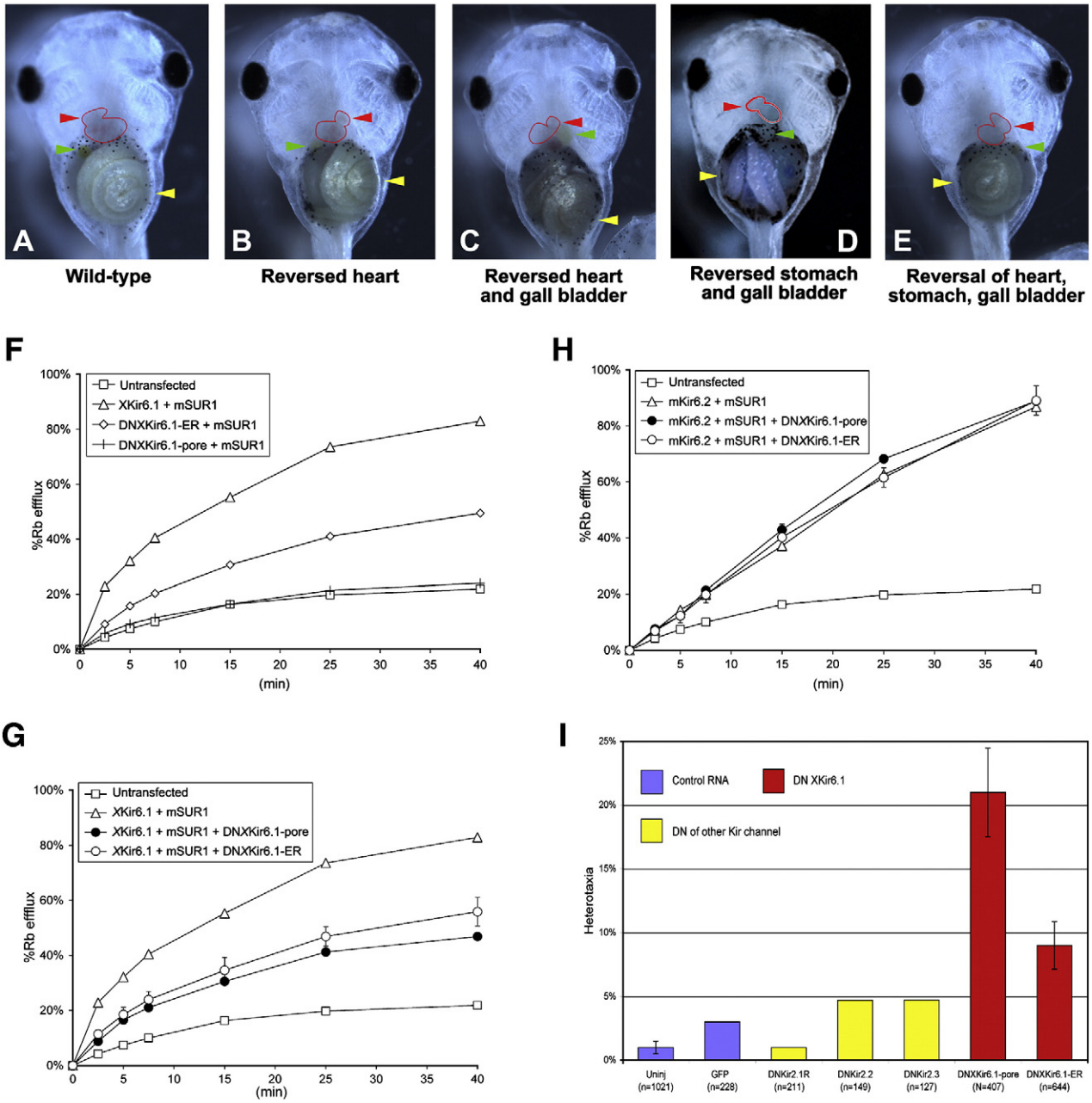

Fig. 1. The K_{ATP} channel is necessary for correct left–right patterning. A) Untreated embryo exhibiting normal *situs* (*situs solitus*). B–E) Embryos treated with K_{ATP} channel blocker HMR-1098 (1.45 mM) (Dhein et al., 2000; Edwards et al., 2009; Jovanovic and Jovanovic, 2005; Light et al., 2001; Suzuki et al., 2003) from Stage 1 cell to Stage 16 (then washed out into 0.1× MMR and allowed to develop to Stage 46 before being scored for organ *situs*) exhibit heterotaxia, including B) reversed heart C) reversed heart and gall bladder D) reversed stomach and gall bladder E) Reversed heart, stomach and gall bladder. F–G) Rubidium flux assays of COSm6 cells expressing various K_{ATP} subunits. F) xKir6.1 with mouse SUR1 (mSUR1) dramatically increased the rate of efflux compared to untransfected cells by about four-fold, suggesting the formation of function K_{ATP} channels. Expression of DNxKir6.1-pore or DNxKir6.1-ER with mouse SUR1 (mSUR1) show that the ER mutant is able to conduct K^+ currents with mSUR1, whilst the pore mutant is non-conductive. G,H) DNxKir6.1-pore and DNxKir6.1-ER knock down activity of K_{ATP} channels consisting of WTxKir6.1 and mouse SUR1 (F), but not those consisting of mouse Kir6.2 and mouse SUR1 (G). I) Injection of dominant-negatives against xKir6.1 causes significant levels of heterotaxia, but not injection of GFP, or dominant-negative mRNAs against other Kir channels DNKir2.1 (Zobel et al., 2003), DNKir2.2 (Zobel et al., 2003) and DNKir2.3 (Bannister et al., 1999).

negative (DN) mutants against the pore-forming subunit of the *Xenopus* K_{ATP} channel. DNxKir6.1-pore has a mutation in its pore-loop motif, which acts as a DN when co-expressed with endogenous subunits (Lalli et al., 1998; Tinker et al., 1996; van Bever et al., 2004). DNxKir6.1-ER is a mutant of xKir6.1 fused to an endoplasmic reticulum (ER)-retention motif (see Materials and methods). A DN effect of ER-retained mutants on oligomeric complexes has been successfully used in functional studies (Kang et al., 2009; Zerangue et al., 1999).

We ensured that these DNs reduced K_{ATP} activity using a Rb^+ flux assay, in which Rb^+ serves as a surrogate for K^+ (Figs. 1F–H). Non-transfected COSm6 cells show a low basal rate of K^+ efflux (Fig. 1F). Expression of DNxKir6.1-pore or DNxKir6.1-ER with mouse SUR1 (mSUR1) show that the ER mutant conducts K^+ currents with mSUR1, whilst the pore mutant is non-conductive (Fig. 1F). Co-expression of xKir6.1 with mouse SUR1 (mSUR1) dramatically increased the rate of efflux compared to untransfected cells by about four-fold, suggesting the formation of function K_{ATP} channels (Fig. 1G). Co-expression of either DNxKir6.1-pore or DNxKir6.1-ER with xKir6.1 and mouse SUR1 decreased K^+ efflux by about 43% at the 45 min time-point for DNxKir6.1-pore and by about 33% for DNxKir6.1-ER (Fig. 1G), suggesting that these constructs indeed act as dominant-negatives against K_{ATP} channels formed with xKir6.1 and mouse SUR1. The DNs did not disrupt K_{ATP} channels formed with mouse Kir6.2 and SUR1 (Fig. 1H), showing that they are specific against K_{ATP} channels comprising Kir6.1.

We injected each DN mRNA into one-cell *Xenopus* embryos, and scored them for LR asymmetry at stage 46. DNxKir6.1-pore and DNxKir6.1-ER both caused statistically significant rates of heterotaxia (21% and 9% respectively, $p<0.01$), while numerous control injections (dominant-negatives against Kir2.1 (Zobel et al., 2003), Kir2.2 (Zobel et al., 2003) and Kir2.3 (Bannister et al., 1999), and GFP and β-galactosidase mRNA) were without effect (Fig. 1I).

Thus, inhibition of the K_{ATP} channel via several K_{ATP} blockers, and molecular knockdown of xKir6.1 (but not of closely-related K_{ir} channels) via two different DN strategies, both cause significant heterotaxia in *Xenopus* embryos. We conclude that functional K_{ATP} channels are necessary for correct LR patterning in *Xenopus*.

K_{ATP} functions at both early and late cleavage stages in LR patterning

In order to determine when K_{ATP} functions in LR patterning, we incubated embryos in the K_{ATP} blocker, HMR-1098 (Dhein et al., 2000; Edwards et al., 2009; Gogelein et al., 2000; Gogelein et al., 2001; Kaab et al., 2003; Light et al., 2001; Suzuki et al., 2003), that caused the highest rate of heterotaxia in our initial screen (Supplement 1), over different time intervals. Embryos were placed into HMR-1098 starting at different times, washed thoroughly at Stage 19, allowed to develop to Stage 46, and then scored for heterotaxia. We found that embryos from different mothers often exhibited significantly different responses in these experiments (Fig. 2A), and hence scored embryos from each mother separately.

Embryos that were incubated in HMR-1098 blocker starting from either one cell stage or stage 7–8.5 showed significant levels of heterotaxia (Fig. 2A). This suggests that K_{ATP} functions in LR patterning at both very early cleavage stages, and at a time period just before the mid-blastula transition (stage 7–8), (Newport and Kirschner, 1982a,b).

Some components of the laterality pathway function asymmetrically, such that LR patterning defects are only observed when knockdown or overexpression of the gene occurs on one side (Toyoizumi et al., 2005). Hence, we injected embryos with DN mRNA on either the left or right side at 4-cell stage, with β-galactosidase (β-gal) mRNA as a lineage tracer to enable retrospective staining and sorting, then scored them for

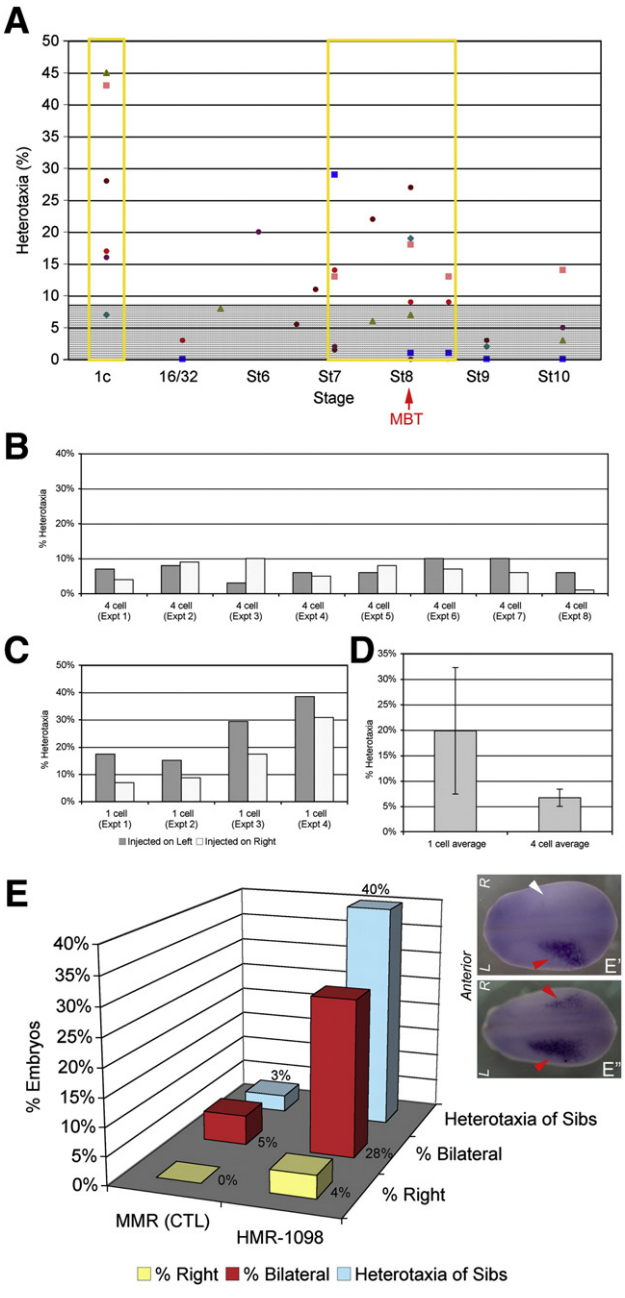

Fig. 2. The K_{ATP} channel functions in both early and late cleavage in LR patterning, and signals to the left-sided Nodal signaling cascade. A) Embryos were incubated in K_{ATP} channel blocker HMR-1098 starting from the indicated stages, and washed out at ~Stage 19. Each differently-colored dot represents embryos from a different mother. The gray shaded area on the chart indicates 9% heterotaxia, which is the level of heterotaxia required in a dish of 100 embryos to achieve significance of heterotaxia over a dish of controls with 2% heterotaxia in a chi-squared test. Significant rates of heterotaxia were observed when embryos were incubated in HMR-1098 starting from one cell, and from about Stage 7 to Stage 8.5. MBT, mid-blastula transition (see text for details). B) Dominant-negative xKir6.1-pore does not cause significantly different rates of heterotaxia when it is injected on the left versus the right side of the embryo at four cell (difference is not significant, $p>0.6$ by paired t-test). C) When asymmetric injections were repeated at one cell, it was found that injection on the left gives a consistently higher rate of heterotaxia than injection on the right, and left injected embryos exhibit a consistently higher rate of heterotaxia than right-injected embryos in every experiment ($p<0.01$ by paired t-test). D) Injections in one half of the embryo at one cell causes approximately 3× as many embryos with heterotaxia as compared to injections in one half of the embryo at four cell, showing that the K_{ATP} channel has a role in LR patterning at the earliest cleavage stages. E) K_{ATP} channel blocker HMR-1098 randomizes Nodal. Wild-type embryos typically exhibit Nodal expression only on the left side of the embryo (E′). Control embryos incubated in 0.1× MMR media alone exhibited only 4% incorrect Nodal staining (right-sided or bilateral staining), and control sibling embryos exhibited a similar 3% rate of background heterotaxia. However, embryos incubated in HMR-1098 exhibited 33% right-sided (image not shown) and bilateral Nodal staining (E″), compared to the 40% rate of heterotaxia seen in sibling embryos incubated in HMR-1098 (E).

LR patterning defects at stage 46. WT and heterotaxic embryos were then fixed and stained for β-gal to confirm the sidedness of the original injection. We found that embryos injected at 4-cell exhibited the same level of heterotaxia whether they were injected into the left or right sides, suggesting that K_{ATP} channel functions bilaterally at later stages (Fig. 2B).

We next asked whether the earlier (prior to the 4-cell stage) role of K_{ATP} may be unilateral. Since the cleavage and pigment differences that allowed us to distinguish L and R at 4-cell stage were not present at stage 1, embryos were injected at the 1-cell stage, off center, again with (β-gal) mRNA as a lineage tracer to enable retrospective staining and sorting. Because the embryos were injected off center, they most often received the DN only on one side of the first cleavage plane, which usually divides the embryo into left and right (Klein, 1987; Masho, 1990). Similarly, injection of only one cell at the 2-cell stage is routinely used to target half the embryo, allowing the untreated contralateral half to serve as an internal control (Harvey and Melton, 1988; Vize et al., 1991; Warner et al., 1984). Staining for β-gal and post-sorting allowed us to determine which half received DN mRNA. Strikingly, embryos injected on the left side were consistently and significantly more likely to develop heterotaxia than those that had been injected on the right side ($p<0.01$ by paired t-test) (Fig. 2C). Thus, we conclude that, in contrast to the later stages, the early period of K_{ATP} function is asymmetric, taking place on the left side.

Taken together, the pharmacological and timed injection results suggest that K_{ATP} has two separate roles in laterality: a very early, LR-asymmetric role, and a later bilateral role.

K_{ATP} channel function is upstream of the left-sided Nodal signaling cascade

The left-sided Nodal signaling cascade is a highly conserved step in LR patterning (Boorman and Shimeld, 2002). Hence, we asked whether disruption of K_{ATP} activity alters left-sided *Nodal* expression. Only 5% of control embryos exhibited incorrect Nodal expression (right-sided or bilateral staining; $n=57$) when assayed by *in situ* hybridization, comparable to the 3% rate of organ heterotaxia seen in sibling embryos (Fig. 2E). In contrast, embryos incubated with HMR-1098 from the one cell stage to Stage 19 exhibited 28% incorrect *Nodal* staining (non-left-sided expression), and siblings of these HMR-1098 embryos exhibited 40% heterotaxia ($n=25$; Fig. 2E). We conclude that K_{ATP} functions upstream of the left-sided transcription of Nodal.

Localization of Kir6.1 protein in LR-relevant developmental stages

In order to gain insight into the function of K_{ATP} in LR patterning, we characterized K_{ATP} localization in embryos during the relevant stages. To test the specificity of an anti-Kir6.1 antibody, xKir6.1 was fused to a short myc epitope tag (xKir6.1-myc), and injected into one-cell *Xenopus* embryos. Lysates of injected embryos were collected at Stage 11 (one day later), after allowing the injected mRNA to be translated to detectable levels, and probed with anti-myc (Campbell et al., 1992; Hu et al., 1995) or anti-Kir6.1 (Foster et al., 2008) in Western blotting. Both antibodies recognized the protein product of the injected mRNA, at molecular weights ~60-, ~120-, ~180-kDa and higher (Fig. 3A, lanes 2 and 5), indicative of specific multiples of the monomeric band. This suggests that the injected xKir6.1-myc fusion protein was forming multimers, as expected of an oligomeric channel. Therefore, the anti-Kir6.1 antibody, which specifically recognizes a myc-tagged xKir6.1 protein, recognizes xKir6.1. We hence used this antibody to probe endogenous xKir6.1.

Western blotting with anti-Kir6.1 against uninjected one-cell *Xenopus* lysates indicated two bands, at ~40- and ~60-kDa (lane 7). (The ~40 kDa band is not recognized by anti-myc in xKir6.1-myc-injected embryos, and may be a non-specific band or an xKir6.1 splice variant present in early embryos). The ~60 kDa band is close to the 51 kDa size for Kir6.1 (Foster et al., 2008; Suzuki et al., 1997). Importantly, the detected ~60-kDa band ran at about the same size as the ~60-kDa band produced by the overexpressed xKir6.1-myc. The identification of Kir6.1 in 1-cell embryos shows that Kir6.1 maternal protein is present from one cell, consistent with an important role in early developmental patterning. Pre-incubation of the antibody with Kir6.1 peptide (lane 8), but not pre-incubation with Kir6.2 peptide (lane 9), completely removed observed bands.

A SUR2-specific antibody (Pu et al., 2008) detected several bands in one-cell *Xenopus* lysates, one of which, at about 130 kDa, is close to the expected size of SUR2A (150 kDa) and may be a splice variant (Fig. 3B).

We carried out immunofluorescence with anti-Kir6.1 and anti-SUR2A, focusing on stages where K_{ATP} plays a role in LR patterning. Western blotting showed that xKir6.1 was present from the one cell (Fig. 3A, lane 7) stage through at least stage 12 (not shown). However, immunofluorescence on sections of embryos from the 2- to 8-cell stage revealed low levels of signal (Figs. 3F, G compare to positive control anti-H/K-ATPase in Fig. 3E), perhaps due to endogenous yolk autofluorescence. At Stage 6, xKir6.1 begins to localize to intracellular domains (green arrows) and to isolated regions on plasma membranes facing the blastocoel (green arrowheads) (Fig. 3H). This pattern continues at stage 7 (Fig. 3I, J), when Kir6.1 localizes to basal membranes surrounding one face of the blastocoel (Fig. 3I, J) as well as to punctate bright spots between cells, particularly near the basal surface (Fig. 3J, blue arrows). Colocalization studies (Figs. 3L–N; shown at Stage 8) show that the intracellular domains recognized by anti-Kir6.1 lie peripheral to the nucleus, consistent with ER localization. At Stage 8, xKir6.1 remains localized to intracellular domains (Fig. 3K, green arrows) and to plasma membrane in many parts of the embryo (Fig. 3K, green arrowheads).

Immunofluorescence with anti-SUR2 in early cleavage *Xenopus* embryos showed punctate, tight junction-like staining during cleavage stages, including at 32/64 cell (Fig. 3O) and two and four cell stages (Figs. 3P–R). Thus, components of K_{ATP} are present in early frog embryos with a cellular localization consistent with channel function.

K_{ATP} currents can be detected in a subpopulation of Xenopus blastomeres

Because of the known role for voltage gradients in LR patterning, and the control of the membrane potential by K_{ATP} in many cell types, we hypothesized that Kir6.1 channels may function in LR by controlling membrane voltage. Sharp electrode voltage measurements in 18 different blastomeres from ten different embryos between the 1-cell stage to St. 6 did not reveal any sensitivity to K_{ATP} channel blocker glibenclamide or opener diazoxide (data not shown). However, at about Stage 7, three of twenty blastomeres measured from ten different embryos responded in a manner typical of K_{ATP} channels, exhibiting the predicted response to combinations of the treatments diazoxide, azide and glibenclamide, e.g. hyperpolarizing in response to diazoxide, depolarizing in response to glibenclamide and repolarizing upon removal of glibenclamide (Fig. 4). This suggests that there are K_{ATP} channel currents in early *Xenopus* embryos. However, this rate of response is uncharacteristically low, suggesting that the channels may lie within inner layers of the embryo, or only within a small domain of cells that may not be electrically coupled to external blastomeres, and hence are undetectable by impalement through external membranes.

K_{ATP} channels do not control asymmetry by modulating blastocoel potassium levels

Maintenance of K^+ composition in the endolymph by K^+-channels is critical for the proper function of the mammalian inner ear (Lang et al., 2007), which uses an H,K-ATPase-Kir4.1-KCNQ1

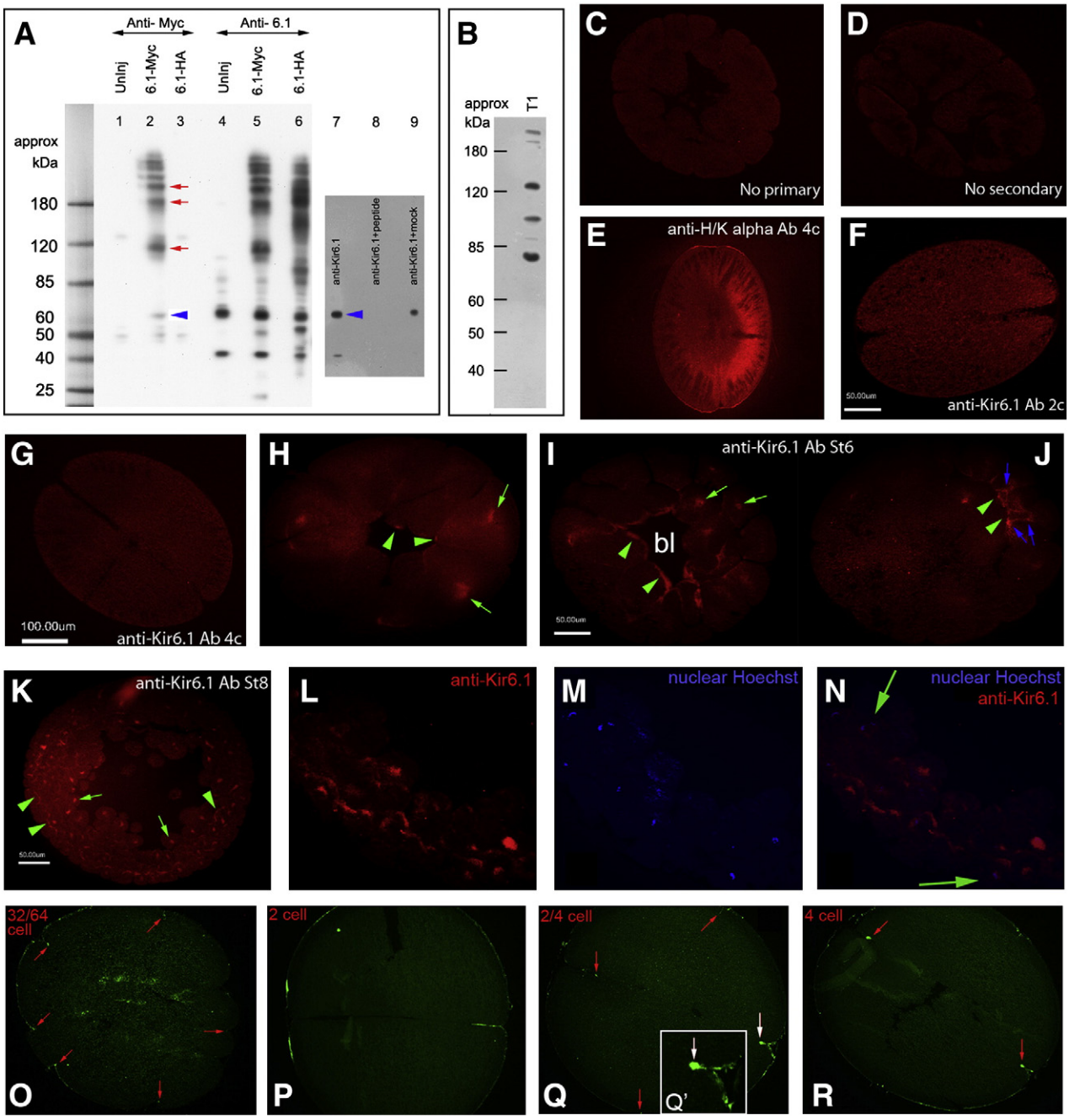

Fig. 3. Immunolocalization of *Xenopus* Kir6.1 and SUR2A. A) Western blotting with anti-myc and anti-Kir6.1 antibodies against lysates from Stage 11 embryos injected at one cell with xKir6.1-myc mRNA. The blot confirms that both antibodies recognize products with molecular weights at multiples of 60 kDa (lanes 2 and 5). Although this is slightly larger than the up to ~51 kDa size recognized for Kir6.1 in other studies (Foster et al., 2008; Suzuki et al., 1997), it runs at the same size as the Kir6.1-myc construct probed with anti-Myc (blue arrow, lane 2), confirming that the anti-Kir6.1 antibody recognizes xKir6.1 protein. The higher molecular weight bands were not observed in lysates from uninjected embryos (lanes 1 and 4). Lysates of uninjected one-cell *Xenopus* embryos shows that 1-cell embryos contain maternal xKir6.1 protein (lanes 4 and 7, blue arrow). Pre-incubation of the antibody with Kir6.1 peptide (lane 8), but not with a Kir6.2 peptide (lane 9), abolished immunoreactive bands. Anti-myc recognized a faint band at about 45-kDa in uninjected embryos (lane 1); this may be endogenous c-myc. B) A SUR2 antibody recognizes several bands in one-cell *Xenopus* lysates, including a 130 kDa band, approximately the size of SUR2 (150 kDa). C–K) Immunofluorescence with anti-Kir6.1 antibody on sections from early to late cleavage stage in *Xenopus* embryos. C) Control sections without primary or (D) secondary antibodies exhibit low level staining and low levels of yolk autofluorescence. E) Positive control anti-H/K-ATPase antibody shows expected left–right asymmetric localization. F, G) At two to four cell stage, xKir6.1 exhibits low levels of expression and indistinct localization. H) At Stage 6, xKir6.1 is localized to intracellular domains (green arrows) and to isolated regions on plasma membranes facing the blastocoel (green arrowheads). I, J) At stage 7, Kir6.1 is localized to intracellular domains (I, green arrows) and membranes on the basal face of animal cap cells lining the blastocoel (J, green arrowheads). Intercellular punctate staining is also observed (J, blue arrows). K) At Stage 8, xKir6.1 remains localized to intracellular domains (K, green arrows) and to plasma membrane in many parts of the embryo (K, green arrowheads). L–N) When intracellular domains recognized by anti-Kir6.1 (L) are co-localized with nuclear DNA (M), they appear to lie peripheral to the nucleus (N), suggestive of endoplasmic reticulum localization. O–R) Immunofluorescence with anti-SUR2A antibody in early cleavage *Xenopus* embryos show punctate, tight junction-like staining at from two cell to stage 32/64 cell. Q′ is a close up of the staining at the junction of a cleaving two to four cell embryo, indicated with a white arrow in Q.

circuit similar to that found in early frog LR patterning (Aw et al., 2008b; Marcus et al., 2002; Shibata et al., 2006; Van Laer et al., 2006). Because the xKir6.1 potassium channel is localized to basal membranes surrounding the blastocoel during stage 7 (Figs. 3I, J), we tested the hypothesis that the K_{ATP} channel controls embryonic asymmetry by modulating the potassium currents of the blastocoel.

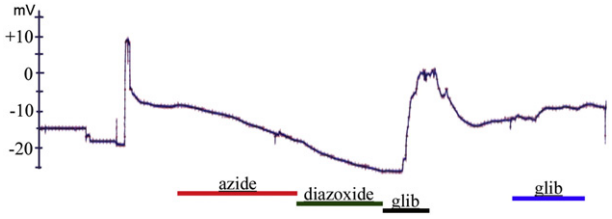

Fig. 4. K_{ATP} channel activity in the early cleavage *Xenopus* embryo is detectable in a few surface blastomeres. Whole-cell electrophysiological recordings from random locations in developing cleavage stage *Xenopus* embryos revealed three of 20 blastomeres impaled that responded in a manner typical of K_{ATP} channels, exhibiting the predicted response to combinations of the treatments diazoxide, azide and glibenclamide, e.g. hyperpolarizing in response to azide, hyperpolarizing in response to diazoxide, depolarizing in response to glibenclamide and repolarizing upon removal of glibenclamide. This figure shows a representative trace of one of the three responding blastomeres.

To determine whether potassium concentration in the blastocoel is important for correct LR patterning, we altered potassium levels in Stage 7 embryos, and assayed LR patterning. We first increased blastocoel potassium by injecting 4 nl of 2.7 M potassium gluconate. In an embryo with blastocoel volume of about 100 nl, this would raise blastocoel potassium by about 25-fold. This did not cause significant rates of heterotaxia (less than 1%). Conversely, we next decreased blastocoel potassium, by injecting up to 4 nl of 2 M K^+-chelator, Kryptofix 2,2,2. This resulted in a final concentration of chelator in the blastocoel of up to 80 mM, more than sufficient to chelate potassium (Beny and Schaad, 2000; Bussemaker et al., 2002). This also did not cause significant heterotaxia (<1%). Our data suggest that blastocoel potassium concentration is not important for LR patterning, and hence this is unlikely to be a mechanism by which K^+ channels function in laterality.

K_{ATP} channels regulate tight junctions in Xenopus

A second possible model for K_{ATP} function in LR was also suggested by our immunofluorescence studies. Anti-SUR2 showed a punctate, tight junction-like localization (Merzdorf et al., 1998) at 2- to 64-cell cleavage stages (Figs. 3O–R). The Kir6.1 antibody also appears to localize to cell–cell junctions and intercellular membranes at about Stage 6 (Figs. 3I, J).

The 3 types of cell–cell junctions, tight junctions, adherens/anchoring junctions, and gap junctions, have all been shown to play important roles in LR patterning (Brizuela et al., 2001; Chuang et al., 2007; Garcia-Castro et al., 2000; Kurpios et al., 2008; Levin and Mercola, 1998b; Levin and Mercola, 1999; Simard et al., 2006; Vanhoven et al., 2006). Interestingly, K_{ATP} channels co-localize with and control tight junction permeability in organs with regulated tight junctions (Jons et al., 2006).

Hence, we tested the hypothesis that K_{ATP} is required for LR asymmetry by regulation of tight junction function in the early embryo. During development, *Xenopus* embryos exhibit tight junctions from the two cell stage (Merzdorf et al., 1998). We used a biotin-labeling assay (Merzdorf et al., 1998) to probe tight junction permeability of cleavage stage embryos that had been injected with K_{ATP} channel DN, DNxKir6.1-pore. After incubation of embryos in Sulfo-NHS-LC-Biotin, a membrane and tight junction impermeant biotin derivative that will only label exposed amines on the embryo surface, embryos were fixed, sectioned and probed with streptavidin-Alexa 555. Embryos were scored as positive for inner membrane staining only if biotin labeling occurred on membranes at least one cell layer deep, as the regular process of cell cleavage of outermost blastomeres during the labeling window may allow biotin to label the second cell layer.

As a positive control, embryos were incubated for 2 h in Ca^{2+}- and Mg^{2+}-free 0.1× MMR, which breaks tight junctions and induces cell dissociation. 100% of these embryos exhibited extensive staining of inner membranes (Fig. 5A). Negative control embryos injected with GFP mRNA showed faint staining of inner membranes (rarely more than one cell layer deep) in 19% of the embryos (3/16) (Fig. 5B). In contrast, DNx6.1p-injected embryos showed extensive staining of inner membranes, often several cell layers deep, in 53% (8/15) of embryos (Figs. 5C, D).

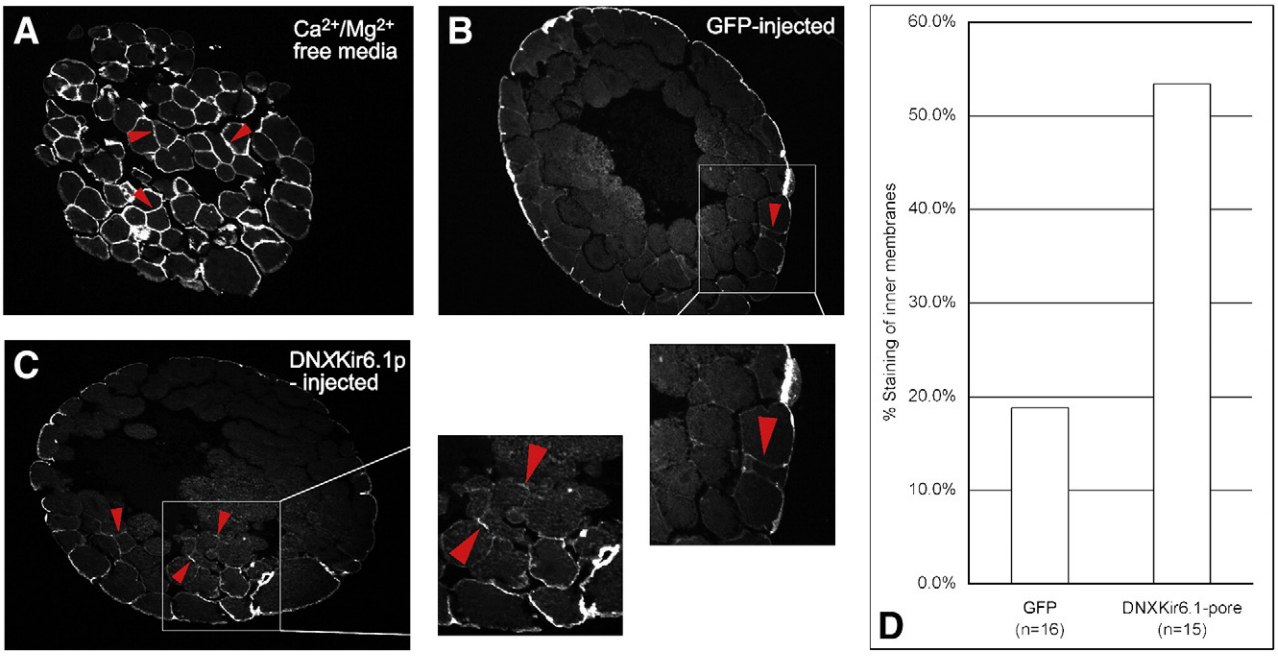

Fig. 5. Dominant-negative DNxKir6.1-pore against the K_{ATP} channel changes tight junction properties of early cleavage stage *Xenopus* embryos. A tight junction and membrane impermeable biotin that labels surface proteins allowed probing of tight junction integrity in *Xenopus* embryos (Merzdorf et al., 1998). A) Incubation of embryos in $Ca2^+$ and $Mg2^+$-free media caused breaking of tight junctions and extensive labeling of inner membranes. B) Control embryos injected with Venus-GFP mRNA showed faint staining of inner membranes, but not more than one cell layer deep (red arrowhead and inset). C) Embryos injected with DNxKir6.1-pore showed extensive staining of inner membranes, often several cell layers deep (red arrowheads and inset). D) In total, 3/16 embryos (19%) injected with control GFP mRNA exhibited staining of membranes one cell layer or more deep, and 8/15 (53%) of embryos injected with DNxKir6.1-pore mRNA exhibited staining of membranes one cell layer or more deep.

These data demonstrate that DNxKir6.1 expression changes the intercellular adhesion properties and/or tight junction integrity of early *Xenopus* embryos. Since K_{ATP} channels have been shown to control tight junctions (Jons et al., 2006), and appropriate functioning of tight junctions is necessary for left–right patterning (Brizuela et al., 2001; Simard et al., 2006; Vanhoven et al., 2006), we propose that K_{ATP} disruption randomizes LR asymmetry via changes in the properties of tight junctions in the early embryo.

K_{ATP} function in the LR pathway is conserved in chick embryogenesis

Several ion channel and pump proteins have been shown to function in LR patterning in chick embryos (Adams et al., 2006b; Levin et al., 2002; Raya et al., 2004). The chick is an important model species for understanding asymmetry because its blastoderm architecture is typical of most mammals. Hence, we wanted to test whether K_{ATP} channel function in LR patterning is conserved to the chick.

Chick Kir6.1 (cKir6.1) is transcribed throughout the early primitive streak in gastrulating chick embryos in a symmetrical manner, at precisely the time at which differential membrane voltage gradients are establishing asymmetric gene expression (Levin et al., 2002) (Figs. 6A, B). In order to test whether K_{ATP} function is important for chick LR asymmetry, we analyzed the expression of a key early left-sided gene, *Sonic hedgehog* (Levin et al., 1995), following bilateral exposure to activators and blockers *in ovo* from st. 1 to st. 5. *Shh* is a standard readout in the chick because it is a known determinant of the highly conserved left-sided *Nodal* domain and subsequent organ *situs* (Levin et al., 1997; Pagan-Westphal and Tabin, 1998).

Whereas embryos exposed to vehicle alone exhibited 94% left-sided *Shh* (Fig. 6C) and only 6% incorrect *Shh* (right-sided, bilateral or no *Shh* expression), bilateral exposure to the K_{ATP} channel blocker repaglinide (Dabrowski et al., 2001; Gromada et al., 1995) randomized expression of *Shh* (Fig. 6D), such that 29% of embryos exhibited incorrect *Shh* expression ($p<0.01$ by chi-squared test). Bilateral exposure to the K_{ATP} channel activator diazoxide (D'Hahan et al., 1999) likewise randomized *Shh*, and also induced expansion of *Shh* expression posteriorly from the node into the mid-streak (Fig. 6E), a unique phenotype not previously described as a consequence of any other known treatment. Thus, the expression of cKir6.1 at the place and time where ionic signaling is being transduced into gene expression changes (Raya et al., 2004), along with the randomization of LR marker *Shh* following pharmacological treatments targeting K_{ATP} channels, are consistent with a role of K_{ATP} channels in chick LR patterning.

Discussion

K_{ATP} channels are involved in left–right patterning

Upstream of asymmetric gene expression, the left–right (LR) patterning pathway in numerous vertebrate and invertebrate model species involves a variety of physiological signals, including calcium fluxes (Schneider et al., 2007), voltage gradients (Adams et al., 2006b;

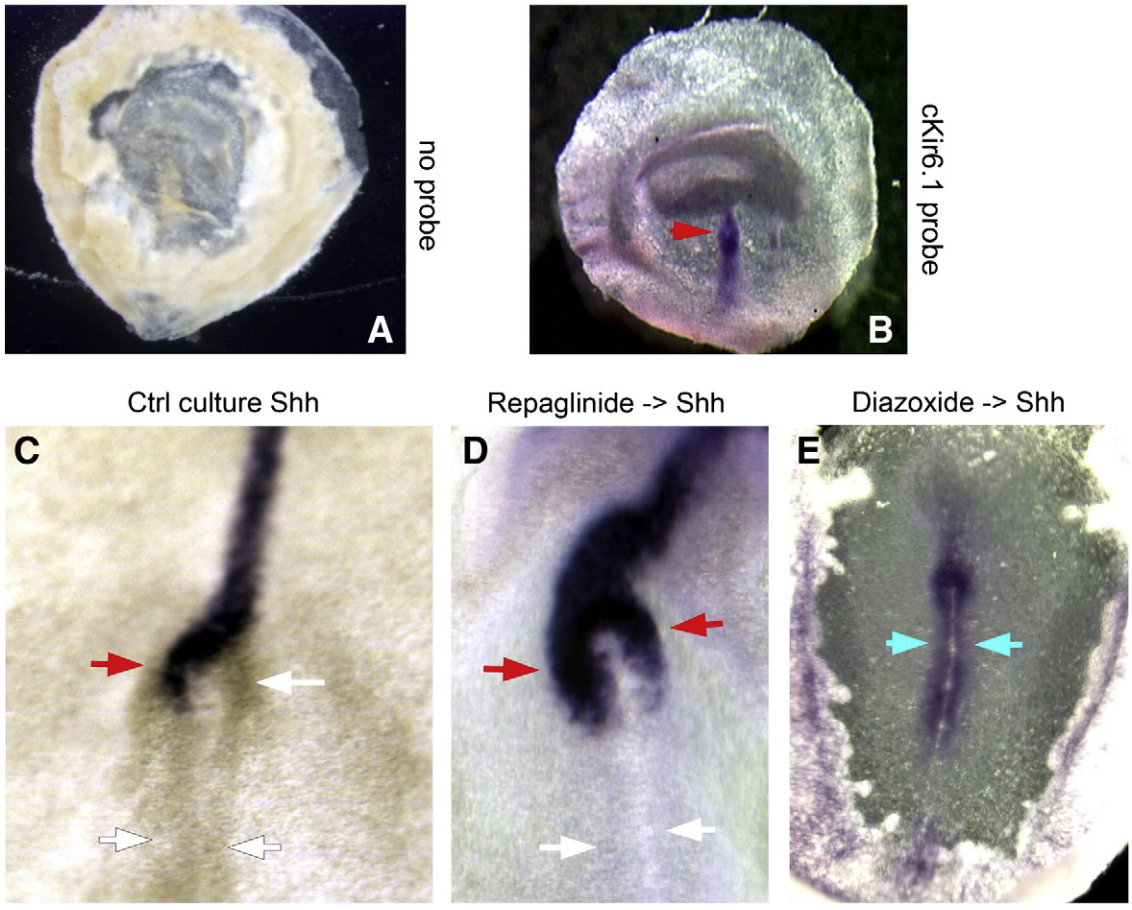

Fig. 6. K_{ATP} function in the LR pathway is conserved in chick embryogenesis. A, B) Chick Kir6.1 is transcribed throughout the early primitive streak in a symmetrical manner, at the time during which differential membrane voltage gradients are establishing asymmetric gene expression (Levin et al., 2002). C) Control embryos exposed to vehicle alone exhibited 94% left-sided *Shh*. D) 29% of embryos exposed bilaterally to 10.6 μM K_{ATP} blocker repaglinide (Dabrowski et al., 2001; Gromada et al., 1995) exhibited randomized expression of *Shh* ($p<0.01$ by chi-squared test). E) Bilateral exposure to 200 μM K_{ATP} activator diazoxide (D'Hahan et al., 1999) randomized *Shh*, also inducing a unique phenotype not known to be observed after any other treatment: expansion of *Shh* expression posteriorly from the node into the mid-streak.

Levin et al., 2002), and flows of endogenous small molecule signals such as inositol polyphosphates (Albrieux and Villaz, 2000; Sarmah et al., 2005) and neurotransmitters (Fujinaga and Baden, 1991; Toyoizumi et al., 1997), via ion channels and pumps. LR-relevant ion transporters include Ca^{2+} channels (Garic-Stankovic et al., 2008; Hibino et al., 2006; McGrath et al., 2003; Pennekamp et al., 2002), KCNJ9 (Aw et al., 2008b) and KCNQ1 (Morokuma et al., 2008) potassium channels, as well as pumps, including the ER Ca^{2+} pump (Kreiling et al., 2008), and H^+ pumps (Adams et al., 2006b), H^+/K^+ exchangers (Levin et al., 2002), and Na^+/K^+ exchangers (Ellertsdottir et al., 2006).

The hierarchical pharmacological screen that led to the identification and molecular validation of several H^+ and K^+ transporters in *Xenopus laevis* (Adams and Levin, 2006a,b) also implicated the K_{ATP} channel (Supplement 1). This screen, which assays the position of 3 internal organs, has a maximum detectable incidence of randomization of 87% (because fully-randomized organs occasionally land in their correct positions by chance, thus being scored as wild-type). Blocking of K_{ATP} caused heterotaxia rates of up to ~50%, comparable to levels seen after knockdown of other proteins involved in LR patterning (Adams et al., 2006a; Hadjantonakis et al., 2008; Kishimoto et al., 2008; Maisonneuve et al., 2009; Morokuma et al., 2008; Yamauchi et al., 2009), suggesting the K_{ATP} channel as a component of LR patterning. The range of heterotaxia rates caused by different blocker drugs is likely a function of both drug efficacy (these drugs were developed in mammals and may have differing efficiency against *Xenopus* K_{ATP} channels) and solubility in aqueous solution. Interestingly, the drug that causes the highest rate of heterotaxia, HMR-1098, is the most water-soluble of all the K_{ATP} drugs used in the screen. Of note, our strict requirement of only analyzing embryos of dorso-anterior index (DAI) = 5 required that we titer all mRNA and blocker reagents to low levels which result in tadpoles with no defects other than randomization. Thus, the penetrance of the observed phenotypes would be significantly higher at higher levels of K_{ATP} inhibition.

A similar assay also implicated K_{ATP} function in chick (Fig. 6), showing that K_{ATP}'s function in LR asymmetry is conserved to at least one other vertebrate species. The chick is a particularly important model system for understanding the evolutionary aspects of asymmetry because it develops in a flat blastodisc typical of most mammals. While physiological mechanisms establishing consistent asymmetries prior to the formation of the chick node have begun to be investigated (Levin et al., 2002), our follow-up experiments focused on the frog system because of the greater accessibility of the early *Xenopus* embryo to electrophysiological experiments. We confirmed the involvement of K_{ATP} channel function using gene-specific dominant-negative constructs (DNs) (Fig. 1). Unlike morpholinos or interfering RNA (RNAi), which cannot directly affect the function of proteins that are already present, DN mutants function at the protein level by assembling with wild-type subunits and abrogating protein function. Hence, once translated, DNs can probe the role of K_{ATP} at the earliest stages of LR, including targeting maternal protein that may not turn over for many cell cycles. This is especially important in light of our findings that maternal xKir6.1 is present from the one cell stage (Fig. 3A).

Our DN mutants against xKir6.1 specifically inhibit the activity of K_{ATP} channels comprising *x*Kir6.1 (Fig. 1G), but not those comprising mouse Kir6.2 (Fig. 1H). It is still debated as to whether heteromeric K_{ATP} channels consisting of both Kir6.1 and Kir6.2 occur in native tissues (Kono et al., 2000; Pountney et al., 2001; Seharaseyon et al., 2000), and our data suggests that, in our system, Kir6.1 and Kir6.2 do not oligomerize. These xKir6.1 DN mutants cause significant rates of heterotaxia, corroborating the pharmacological data and indicating that K_{ATP} – and specifically, K_{ATP} channels formed of xKir6.1 – is necessary for LR patterning in *Xenopus laevis*.

K_{ATP} channels are expressed in multiple tissues in adult vertebrates. The Kir6.2 isoform is prominent in striated muscle, pancreatic islet cells and neurons. Loss- or gain-of-function mutations cause congenital hyperinsulinism (Huopio et al., 2002) and diabetes (Gloyn et al., 2004; Koster et al., 2000), respectively. In the latter case, diabetes can also be associated with developmental delay and epilepsy, due to aberrant neuronal activity (Gloyn et al., 2004). The above data demonstrate a novel function for xKir6.1-based K_{ATP} channels in development. In mammals, the orthologous Kir6.1 isoform is prominent in smooth muscle, and genetic knockout animals exhibit coronary vasospasm due to the loss of hyperpolarizing currents in the coronary vasculature (Miki and Seino, 2005), but to date, there are no reports of developmental abnormalities in these animals.

When does the K_{ATP} channel act in the LR pathway?

By adding the channel inhibitor HMR-1098 at different time points, we probed K_{ATP} channel function beginning at different developmental stages without requiring immediate drug wash-out, since the critical differentiating time period is in the beginning of the time interval, not the end. These experiments in *Xenopus* (Fig. 2A) showed that two periods during development appear to be key for the role of K_{ATP} in LR patterning—the very early cleavage stages, and a time period just prior to the mid-blastula transition. This latter time period is particularly interesting, as very little is known about mechanisms of left–right patterning in *Xenopus* during the stages following physiological activation of ion currents, gap junctions, and serotonergic signaling (Levin, 2006; Levin et al., 2006), but prior to the function of cilia (Schweickert et al., 2007) and asymmetric Nodal transcription (Lohr et al., 1997; Sampath et al., 1997).

In chick, while cleavage-stage mechanisms have not been probed, a post-gastrulation cascade of asymmetric signaling factors is known upstream of asymmetric Nodal transcription (reviewed in Levin, 1998). While further characterization will be required to determine whether differential K_{ATP} activity is responsible for the different transmembrane potential observed on the L and R sides of the primitive streak (Levin et al., 2002), our data suggest that the role of K_{ATP} is upstream of *Shh* expression at stage 4, and takes place during or prior to other known roles of ion transport in directing subsequent asymmetric gene expression (Fig. 6). As with the H,K-ATPase and V-ATPase, the radically different embryonic architecture between the cleavage-stage frog and the chick blastoderm makes it likely that while the function of these transporters are conserved, the precise mechanism by which they establish the LR-relevant gradients may differ (Levin, 2006; Speder et al., 2007). The randomization of *Shh* expression by global applications of both K_{ATP} inhibitors and activators, suggest that differential (asymmetric) activity of K_{ATP} channels on the left and right sides of the chick embryo is crucial. However, the symmetric expression suggests that this differential activity must arise at the translational level or at the level of gating of mature channel proteins.

The early timing of the first phase of K_{ATP} activity in the LR pathway in frog is underscored by our DN experiments, since the rate of heterotaxia (average ~7%) observed in embryos injected at four cell, though statistically significant in our large sample sizes, was much lower than the rate seen in embryos injected at one cell (~ 20%, Fig. 2D), even though in both cases, ~1 ng of mRNA was injected into each embryo. Because it takes ~1 h for injected mRNA to be translated into protein (based on our observations using reporter mRNAs (Aw et al., 2008a)), injection of DN at one cell will result in knockdown of the channel starting from around two to four cell stage. Similarly, injections of the DN at four cell should result in knockdown starting at about 8–16/32 cell. While the precise profile of mutant protein level vs. time in living embryos is unknown, these data clearly indicate a function for K_{ATP} in the LR signaling pathway that is completed during the first few cleavage stages, since equivalent injections at the 4-cell stage are too late to perturb it.

The fact that K_{ATP} is necessary for LR patterning at early stages is consistent with our finding that the loss of K_{ATP} channel activity leads to randomization of Nodal expression. Thus, the early events controlled by K_{ATP} feed into asymmetry through the conserved *Nodal*-mediated cascade.

How do K_{ATP} channels signal to downstream LR pathway components?

A variety of LR patterning molecules exert their effects by unilateral activity. Examples include *Sonic hedgehog* and *Activin* (Levin et al., 1995), serotonin (Fukumoto et al., 2005), Zic-3 (Kitaguchi et al., 2000), and Vg1 (Hyatt and Yost, 1998). This is true of the K_{ATP} channel at the early period (1–4 cell) of its functioning, since the DNxKir6.1-pore has a greater effect when injected on the left side (Fig. 2C). However, other LR pathway components are not asymmetric in their localization; these include gap junctions (Levin and Mercola, 1998b) and syndecans (Kramer et al., 2002). Similarly, the later period of K_{ATP} channel activity (Stage 6.5–8) shows no evidence of sidedness in either chicken or *Xenopus*. This observation is compatible with a role for the K_{ATP} channel in regulating tight junctions (see below), as tight junctions occur relatively symmetrically and uniformly around the frog embryo (Merzdorf et al., 1998; Sanders and Dicaprio, 1976).

What is the direct physiological function of K_{ATP} in the LR pathway? We used whole-cell electrophysiology to measure K_{ATP} currents, and detected channel activity to a limited extent. However, unlike for the H^+,K^+-ATPase and V-ATPase (Adams et al., 2006b; Levin et al., 2002), consistent asymmetric effects on ion flux or transmembrane potential in early embryos could not be observed. Whole-cell electrophysiology is a very robust assay, and our minimal ability to detect K_{ATP} currents was surprising. However, in light of our immunofluorescence results (Fig. 3), which show xKir6.1 localized to inner membranes and cell junctions in the embryo, a likely interpretation of our data is that K_{ATP} channels in cleavage-stage *Xenopus* embryos lie in domains that may not be electrically coupled to all external blastomeres accessible to microelectrode recordings. Another possibility is that the K_{ATP} channel functions in LR asymmetry by a mechanism other than regulation of membrane voltage. Non-ion conducting functions for ion channels have been demonstrated for several channels, including potassium channels (reviewed in Kaczmarek, 2006). For example, sodium channel β subunits are themselves cell adhesion molecules (CAMs) that mediate cell adhesion by interacting with other CAMs (Malhotra et al., 2000; McEwen and Isom, 2004).

From our immunofluorescence data and previous work demonstrating K_{ATP} regulation of tight junctions (Jons et al., 2006), we hypothesized that K_{ATP} channels might regulate tight junction function in *Xenopus* embryos. Indeed, a biotin assay of tight junction function (Merzdorf et al., 1998) showed that injection of DNxKir6.1-pore alters tight junction integrity in the cleaving embryo, when K_{ATP} functions in LR patterning (Fig. 5). 53% of embryos exhibited breakage of junctional integrity; although this is lower than the degree of tight junction collapse exhibited by embryos incubated in Ca^{2+}- and Mg^{2+}-free media (100%), the incomplete penetrance is not surprising, as mRNA injections will be more mosaic in nature than incubation in aqueous solution, and mRNA levels are titered down to levels that allow normal overall embryo development, in order to score LR-specific phenotypes. A functional role for K_{ATP} channels in inner membranes at tight junctions is consistent with the low detection of K_{ATP} channel activity in surface blastomeres (Fig. 4), since changes in tight junctions can alter electrical coupling between cells in ways that are not robustly detected at the surface. Also, uniform presence of tight junctions throughout the embryo would explain why K_{ATP} expression is not LR-asymmetric at these later stages.

Although this model links K_{ATP} to a significant body of work establishing the role of cell junctions in LR asymmetry (Brizuela et al., 2001; Chuang et al., 2007; Garcia-Castro et al., 2000; Kurpios et al., 2008; Levin and Mercola, 1998b; Levin and Mercola, 1999; Simard et al., 2006; Vanhoven et al., 2006), it also raises additional important questions: 1) Why are cell junction proteins important for LR patterning, and 2) How do K_{ATP} channels regulate tight junctions?

One model of LR patterning, involving asymmetric morphogen transport across gap junctions down an intraembryonic electrical gradient (Adams et al., 2006a; Esser et al., 2006), would require functioning tight junctions. Because tight junctions hold cells together, they provide robust support for gap junction contacts to ensure a continuous electrical circuit. Tight junctions also prevent water from the extracellular medium from entering between cells (Fig. 7A), preventing short circuit and leakage of the electrochemical gradient (Fig. 7A′). Breaking of tight junctions (Fig. 7B) would cause dissipation of the potential gradient, hence disrupting the driving force that initiates LR patterning (Fig. 7B′). The role of tight junctions in regulation of the cytoskeleton (Lockwood et al., 2008; Van Itallie et al., 2009) is also intriguing, as the cytoskeleton is critical for the establishment of asymmetries of left–right protein determinants (Aw et al., 2008a; Morokuma et al., 2008; Qiu et al., 2005).

How does K_{ATP} regulate tight junction integrity? Although several ion channels have been implicated in the regulation of tight junction function (reviewed in Rajasekaran et al., 2008), including K_{ATP} (Jons et al., 2006), the mechanisms involved remain elusive. Tight junction function is highly regulated by multiple signaling networks (Matter and Balda, 2003). One possibility is that ionic changes could cause alterations in the phosphorylation states of tight junction proteins (Marshall et al., 1999). Another possibility is that conformational changes associated with K_{ATP} channel gating could signal to tight junction regulatory molecules (Hegle et al., 2006). It has been shown that overexpression of the tight junction protein claudin alters cell adhesion properties of tight junctions in *Xenopus*, and induces LR patterning defects in both *Xenopus* and chick (Brizuela et al., 2001; Simard et al., 2006). Hence, it is possible that disruption of K_{ATP} causes an upregulation of claudin that leads to alterations in tight junction function. Finally, although we have shown that dominant-negative *x*Kir6.1 alters the integrity of cell–cell contacts important in left–right patterning, we cannot rule out the possibility that it also exerts effects on other key early processes in LR, including gap junctional communication and serotonin transporter activity.

Conclusions

We have identified a new role for the K_{ATP} channel as a component of embryonic left–right patterning. In *Xenopus*, it acts during a period of time when relatively little is known about laterality determination mechanisms — after the earliest steps that set up differences among L and R blastomeres, but prior to later events such as asymmetric gene expression. This intriguing timing of action suggests that it could link the earliest physiological steps in LR patterning to downstream pathways like the left-sided *Nodal* signaling cascade. While effects on membrane potential cannot be completely ruled out, it appears to function by exerting effects on tight junction integrity, a property of crucial importance to voltage- and planar cell-polarity-based mechanisms for coordinating cell orientation within the blastoderm. Our experiments in the chick suggest that the role of the biomedically-important K_{ATP} in LR patterning may be conserved to other organisms, providing another fascinating example of the same molecular components being used to impose spatial patterning upon embryos of radically different developmental architecture. Future work will address the mechanistic details of tight junction-dependent spread of laterality information during embryogenesis. Understanding the synthesis of the physiological, biophysical, and transcriptional events that reliably pattern the third axis in a world that does not macroscopically distinguish left from right will have profound ramifications for developmental, cell, and evolutionary biology as well as biomedicine.

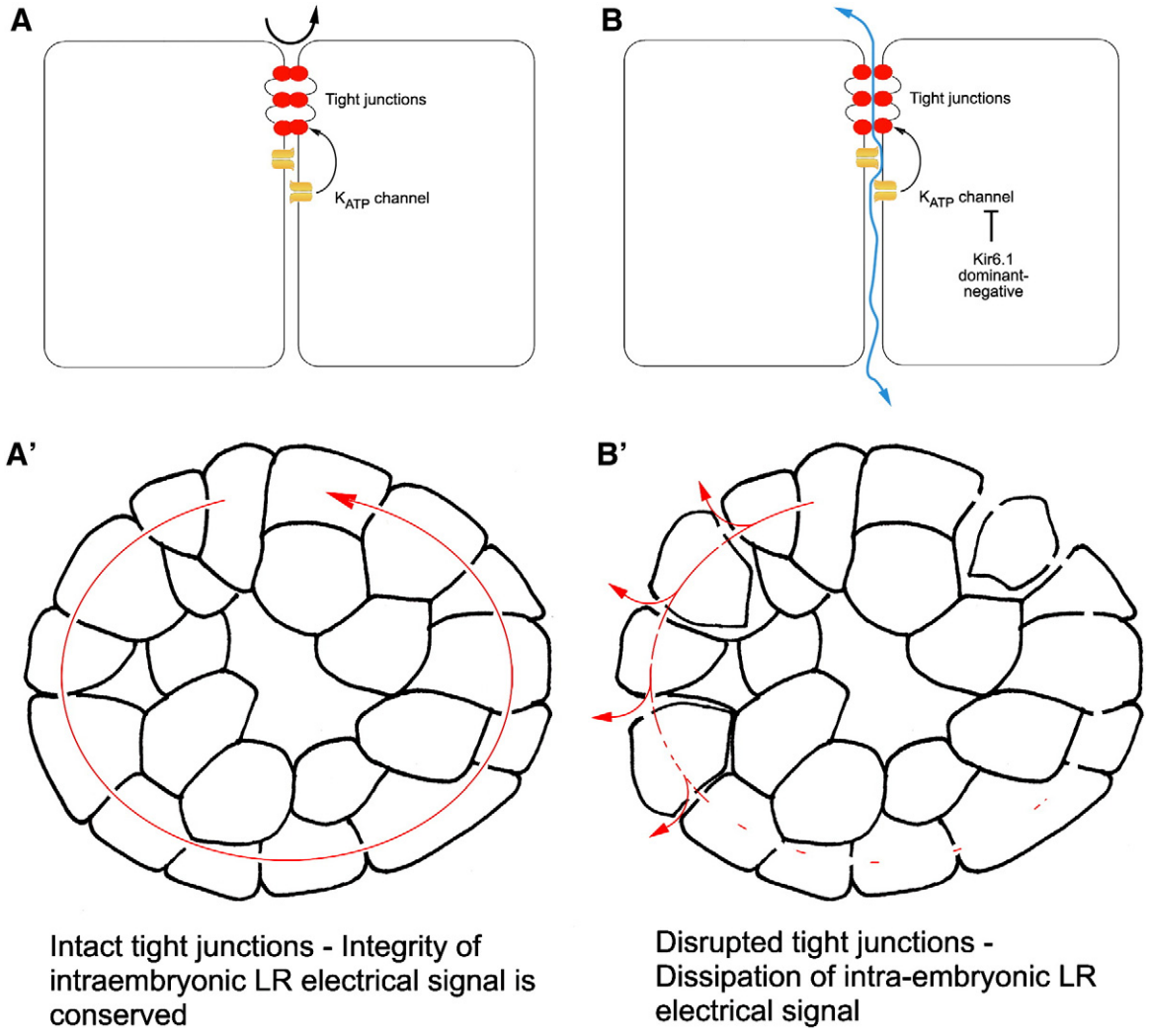

Fig. 7. A model of how disruption of tight junctions by the K_{ATP} channel might cause defects in LR patterning. A) In a normal embryo, tight junctional integrity is conserved in the presence of functional K_{ATP} channels, preventing paracellular flow and leakage (black arrow). A′) In the context of the embryo, functionally robust tight junctional seals would support proper gap junction function and prevent short circuit caused by paracellular leakage, allowing conservation of the intraembryonic LR electrical signal (see text for details). B) The disruption of K_{ATP} channels by xKir6.1 dominant-negatives causes loss of tight junctional integrity and hence paracellular leakage (blue arrow), which would alter both transepithelial potentials, and secondarily, transmembrane voltage gradients in the blastomeres. B′) Disruption of tight junctions is predicted to cause rapid dissipation of the intraembryonic LR electrical signal.

Acknowledgments

We thank Ivy Chen and current members of the Levin lab for many useful discussions. We are grateful to Blanche Schwappach, Asipu Sivaprasadarao, and Frances Ashcroft for their expert advice regarding K_{ATP} molecular and cell biology. We also thank H. Gögelein for HMR-1098 compound, Peter Backx for DNKir2.1 and DNKir2.2 constructs, and D. Wray for DNKir2.3 construct. ML gratefully acknowledges funding support from the NIH (R01-GM077425) and the American Heart Association (Established Investigator Grant 0740088N); SAW was supported by the A*STAR overseas National Science Scholarship from the Agency for Science and Technology (Singapore); NQS is supported by NIH (HL093626) and the American Heart Association (0630268N).

Appendix A. Supplementary data

Supplementary data associated with this article can be found, in the online version, at 10.1016/j.ydbio.2010.07.011.

References

Adams, D.S., Levin, M., 2006a. Inverse drug screens: a rapid and inexpensive method for implicating molecular targets. Genesis 44, 530–540.
Adams, D.S., Levin, M., 2006b. Strategies and techniques for investigation of biophysical signals in patterning. In: Whitman, M., Sater, A.K. (Eds.), Analysis of Growth Factor Signaling in Embryos. Taylor and Francis Books, pp. 177–262.
Adams, D.S., Robinson, K.R., Fukumoto, T., Yuan, S., Albertson, R.C., Yelick, P., Kuo, L., McSweeney, M., Levin, M., 2006a. Early, H+-V-ATPase-dependent proton flux is necessary for consistent left–right patterning of non-mammalian vertebrates. Development 133, 1657–1671.
Adams, D.S., Robinson, K.R., Fukumoto, T., Yuan, S., Albertson, R.C., Yelick, P., Kuo, L., McSweeney, M., Levin, M., 2006b. Early, H+-V-ATPase-dependent proton flux is necessary for consistent left–right patterning of non-mammalian vertebrates. Development 133, 1657–1671.
Albrieux, M., Villaz, M., 2000. Bilateral asymmetry of the inositol trisphosphate-mediated calcium signaling in two-cell ascidian embryos. Biol. Cell 92, 277–284.
Ashcroft, F.M., Harrison, D.E., Ashcroft, S.J., 1984. Glucose induces closure of single potassium channels in isolated rat pancreatic beta-cells. Nature 312, 446–448.
Ashford, M.L., Sturgess, N.C., Trout, N.J., Gardner, N.J., Hales, C.N., 1988. Adenosine-5′-triphosphate-sensitive ion channels in neonatal rat cultured central neurones. Pflugers Arch. 412, 297–304.
Aw, S., Adams, D.S., Qiu, D., Levin, M., 2008a. H, K-ATPase protein localization and Kir4.1 function reveal concordance of three axes during early determination of left–right asymmetry. Mech. Dev. 125, 353–372.

Aw, S., Adams, D.S., Qiu, D., Levin, M., 2008b. H, K-ATPase protein localization and Kir4.1 function reveal concordance of three axes during early determination of left–right asymmetry. Mech. Dev. 125, 353–372.
Aw, S., Levin, M., 2008. What's left in asymmetry? Dev. Dyn. 237, 3453–3463.
Aw, S., Levin, M., 2009. Is left–right asymmetry a form of planar cell polarity? Development 136, 355–366.
Bannister, J.P., Young, B.A., Sivaprasadarao, A., Wray, D., 1999. Conserved extracellular cysteine residues in the inwardly rectifying potassium channel Kir2.3 are required for function but not expression in the membrane. FEBS Lett. 458, 393–399.
Basu, B., Brueckner, M., 2008. Cilia: multifunctional organelles at the center of vertebrate left–right asymmetry. Curr. Top. Dev. Biol. 85, 151–174.
Beny, J.L., Schaad, O., 2000. An evaluation of potassium ions as endothelium-derived hyperpolarizing factor in porcine coronary arteries. Br. J. Pharmacol. 131, 965–973.
Bienengraeber, M., Olson, T.M., Selivanov, V.A., Kathmann, E.C., O'Cochlain, F., Gao, F., Karger, A.B., Ballew, J.D., Hodgson, D.M., Zingman, L.V., Pang, Y.P., Alekseev, A.E., Terzic, A., 2004. ABCC9 mutations identified in human dilated cardiomyopathy disrupt catalytic KATP channel gating. Nat. Genet. 36, 382–387.
Boorman, C.J., Shimeld, S.M., 2002. The evolution of left–right asymmetry in chordates. Bioessays 24, 1004–1011.
Brizuela, B.J., Wessely, O., De Robertis, E.M., 2001. Overexpression of the Xenopus tight-junction protein claudin causes randomization of the left–right body axis. Dev. Biol. 230, 217–229.
Brown, N.A., Wolpert, L., 1990. The development of handedness in left/right asymmetry. Development 109, 1–9.
Burdine, R., Schier, A., 2000. Conserved and divergent mechanisms in left–right axis formation. Genes Dev. 14, 763–776.
Bussemaker, E., Wallner, C., Fisslthaler, B., Fleming, I., 2002. The Na–K-ATPase is a target for an EDHF displaying characteristics similar to potassium ions in the porcine renal interlobar artery. Br. J. Pharmacol. 137, 647–654.
Campbell, A.M., Kessler, P.D., Fambrough, D.M., 1992. The alternative carboxyl termini of avian cardiac and brain sarcoplasmic reticulum/endoplasmic reticulum Ca(2+)-ATPases are on opposite sides of the membrane. J. Biol. Chem. 267, 9321–9325.
Chuang, C.F., Vanhoven, M.K., Fetter, R.D., Verselis, V.K., Bargmann, C.I., 2007. An innexin-dependent cell network establishes left–right neuronal asymmetry in C. elegans. Cell 129, 787–799.
Chutkow, W.A., Pu, J., Wheeler, M.T., Wada, T., Makielski, J.C., Burant, C.F., McNally, E.M., 2002. Episodic coronary artery vasospasm and hypertension develop in the absence of Sur2 K(ATP) channels. J. Clin. Invest. 110, 203–208.
D'Hahan, N., Moreau, C., Prost, A.L., Jacquet, H., Alekseev, A.E., Terzic, A., Vivaudou, M., 1999. Pharmacological plasticity of cardiac ATP-sensitive potassium channels toward diazoxide revealed by ADP. Proceedings of the National Academy of Sciences of the United States of America., 96, pp. 12162–12167.
Dabrowski, M., Wahl, P., Holmes, W.E., Ashcroft, F.M., 2001. Effect of repaglinide on cloned beta cell, cardiac and smooth muscle types of ATP-sensitive potassium channels. Diabetologia 44, 747–756.
Danilchik, M.V., Brown, E.E., Riegert, K., 2006. Intrinsic chiral properties of the Xenopus egg cortex: an early indicator of left–right asymmetry? Development 133, 4517–4526.
Danos, M.C., Yost, H.J., 1996. Role of notochord in specification of cardiac left–right orientation in zebrafish and Xenopus. Dev. Biol. 177, 96–103.
Dhein, S., Pejman, P., Krusemann, K., 2000. Effects of the I(K.ATP) blockers glibenclamide and HMR1883 on cardiac electrophysiology during ischemia and reperfusion. Eur. J. Pharmacol. 398, 273–284.
Doyle, D.A., Morais Cabral, J., Pfuetzner, R.A., Kuo, A., Gulbis, J.M., Cohen, S.L., Chait, B.T., MacKinnon, R., 1998. The structure of the potassium channel: molecular basis of K+ conduction and selectivity. Science 280, 69–77.
Duboc, V., Rottinger, E., Lapraz, F., Besnardeau, L., Lepage, T., 2005. Left–right asymmetry in the sea urchin embryo is regulated by nodal signaling on the right side. Dev. Cell 9, 147–158.
Edwards, A.G., Rees, M.L., Gioscia, R.A., Zachman, D.K., Lynch, J.M., Browder, J.C., Chicco, A.J., Moore, R.L., 2009. PKC-permitted elevation of sarcolemmal KATP concentration may explain female-specific resistance to myocardial infarction. J. Physiol.
Ellertsdottir, E., Ganz, J., Durr, K., Loges, N., Biemar, F., Seifert, F., Ettl, A.K., Kramer-Zucker, A.K., Nitschke, R., Driever, W., 2006. A mutation in the zebrafish Na, K-ATPase subunit atp1a1a.1 provides genetic evidence that the sodium potassium pump contributes to left–right asymmetry downstream or in parallel to nodal flow. Dev. Dyn. 235, 1794–1808.
Esser, A.T., Smith, K.C., Weaver, J.C., Levin, M., 2006. Mathematical model of morphogen electrophoresis through gap junctions. Dev. Dyn. 235, 2144–2159.
Ficker, E., Dennis, A.T., Obejero-Paz, C.A., Castaldo, P., Taglialatela, M., Brown, A.M., 2000. Retention in the endoplasmic reticulum as a mechanism of dominant-negative current suppression in human long QT syndrome. J. Mol. Cell. Cardiol. 32, 2327–2337.
Findlay, I., Dunne, M.J., Petersen, O.H., 1985. ATP-sensitive inward rectifier and voltage- and calcium-activated K+ channels in cultured pancreatic islet cells. J. Membr. Biol. 88, 165–172.
Foster, D.B., Rucker, J.J., Marban, E., 2008. Is Kir6.1 a subunit of mitoK(ATP)? Biochem. Biophys. Res. Commun. 366, 649–656.
Fujinaga, M., Baden, J.M., 1991. Evidence for an adrenergic mechanism in the control of body asymmetry. Dev. Biol. 143, 203–205.
Fukumoto, T., Kema, I.P., Levin, M., 2005. Serotonin signaling is a very early step in patterning of the left-right axis in chick and frog embryos. Curr. Biol. 15, 794–803.
Garcia-Castro, M.I., Vielmetter, E., Bronner-Fraser, M., 2000. N-Cadherin, a cell adhesion molecule involved in establishment of embryonic left–right asymmetry. Science 288, 1047–1051.
Garic-Stankovic, A., Hernandez, M., Flentke, G.R., Zile, M.H., Smith, S.M., 2008. A ryanodine receptor-dependent Cai2+ asymmetry at Hensen's node mediates avian lateral identity. Development.
Gloyn, A.L., Pearson, E.R., Antcliff, J.F., Proks, P., Bruining, G.J., Slingerland, A.S., Howard, N., Srinivasan, S., Silva, J.M., Molnes, J., Edghill, E.L., Frayling, T.M., Temple, I.K., Mackay, D., Shield, J.P., Sumnik, Z., van Rhijn, A., Wales, J.K., Clark, P., Gorman, S., Aisenberg, J., Ellard, S., Njolstad, P.R., Ashcroft, F.M., Hattersley, A.T., 2004. Activating mutations in the gene encoding the ATP-sensitive potassium-channel subunit Kir6.2 and permanent neonatal diabetes. N Engl J. Med. 350, 1838–1849.
Gogelein, H., Englert, H., Kotzan, A., Hack, Rudiger, Lehr, K.-H., Seiz, W., Becker, R.H.A., Sultan, E., Scholkens, B.A., Busch, A.E., 2000. HMR 1098: an inhibitor of cardiac ATP-sensitive potassium channels. Cardiovasc. Drug Rev. 18, 157–174.
Gogelein, H., Ruetten, H., Albus, U., Englert, H.C., Busch, A.E., 2001. Effects of the cardioselective KATP channel blocker HMR 1098 on cardiac function in isolated perfused working rat hearts and in anesthetized rats during ischemia and reperfusion. Naunyn Schmiedebergs Arch Pharmacol. 364, 33–41.
Gromada, J., Dissing, S., Kofod, H., Frokjaer-Jensen, J., 1995. Effects of the hypoglycaemic drugs repaglinide and glibenclamide on ATP-sensitive potassium-channels and cytosolic calcium levels in beta TC3 cells and rat pancreatic beta cells. Diabetologia 38, 1025–1032.
Hadjantonakis, A.K., Pisano, E., Papaioannou, V.E., 2008. Tbx6 regulates left/right patterning in mouse embryos through effects on nodal cilia and perinodal signaling. PLoS ONE 3, e2511.
Harland, R.M., 1991. In situ hybridization: an improved whole mount method for *Xenopus* embryos. In: Kay, B.K., Peng, H.B. (Eds.), Xenopus laevis: practical uses in cell and molecular biology, Vol. 36. Academic Press, San Diego, pp. 685–695.
Harvey, R.P., Melton, D.A., 1988. Microinjection of synthetic Xhox-1A homeobox mRNA disrupts somite formation in developing Xenopus embryos. Cell 53, 687–697.
Heginbotham, L., Lu, Z., Abramson, T., MacKinnon, R., 1994. Mutations in the K+ channel signature sequence. Biophys. J. 66, 1061–1067.
Hegle, A.P., Marble, D.D., Wilson, G.F., 2006. A voltage-driven switch for ion-independent signaling by ether-a-go-go K+ channels. Proc. Natl Acad. Sci. USA 103, 2886–2891.
Hibino, T., Ishii, Y., Levin, M., Nishino, A., 2006. Ion flow regulates left–right asymmetry in sea urchin development. Dev. Genes Evol. 216, 265–276.
Hu, Q., Klippel, A., Muslin, A.J., Fantl, W.J., Williams, L.T., 1995. Ras-dependent induction of cellular responses by constitutively active phosphatidylinositol-3 kinase. Science 268, 100–102.
Huopio, H., Shyng, S.L., Otonkoski, T., Nichols, C.G., 2002. K(ATP) channels and insulin secretion disorders. Am. J. Physiol. Endocrinol. Metab. 283, E207–E216.
Hyatt, B.A., Yost, H.J., 1998. The left–right coordinator: the role of Vg1 in organizing left–right axis formation. Cell 93, 37–46.
Jiang, Y., Lee, A., Chen, J., Ruta, V., Cadene, M., Chait, B.T., MacKinnon, R., 2003. X-ray structure of a voltage-dependent K+ channel. Nature 423, 33–41.
Jons, T., Wittschieber, D., Beyer, A., Meier, C., Brune, A., Thomzig, A., Ahnert-Hilger, G., Veh, R.W., 2006. K+ -ATP-channel-related protein complexes: potential transducers in the regulation of epithelial tight junction permeability. J. Cell Sci. 119, 3087–3097.
Jovanovic, S., Jovanovic, A., 2005. High glucose regulates the activity of cardiac sarcolemmal ATP-sensitive K+ channels via 1, 3-bisphosphoglycerate: a novel link between cardiac membrane excitability and glucose metabolism. Diabetes 54, 383–393.
Kaab, S., Zwermann, L., Barth, A., Hinterseer, M., Englert, H.C., Gogelein, H., Nabauer, M., 2003. Selective block of sarcolemmal IKATP in human cardiomyocytes using HMR 1098. Cardiovasc. Drugs Ther. 17, 435–441.
Kaczmarek, L.K., 2006. Non-conducting functions of voltage-gated ion channels. Nat. Rev. Neurosci. 7, 761–771.
Kane, G.C., Behfar, A., Dyer, R.B., O'Cochlain, D.F., Liu, X.K., Hodgson, D.M., Reyes, S., Miki, T., Seino, S., Terzic, A., 2006. KCNJ11 gene knockout of the Kir6.2 KATP channel causes maladaptive remodeling and heart failure in hypertension. Hum. Mol. Genet. 15, 2285–2297.
Kane, G.C., Liu, X.K., Yamada, S., Olson, T.M., Terzic, A., 2005. Cardiac KATP channels in health and disease. J. Mol. Cell. Cardiol. 38, 937–943.
Kang, J.Q., Shen, W., Macdonald, R.L., 2009. The GABRG2 mutation, Q351X, associated with generalized epilepsy with febrile seizures plus, has both loss of function and dominant-negative suppression. J. Neurosci. 29, 2845–2856.
Kishimoto, N., Cao, Y., Park, A., Sun, Z., 2008. Cystic kidney gene seahorse regulates cilia-mediated processes and Wnt pathways. Dev. Cell 14, 954–961.
Kitaguchi, T., Nagai, T., Nakata, K., Aruga, J., Mikoshiba, K., 2000. Zic3 is involved in the left–right specification of the Xenopus embryo. Dev. Suppl. 127, 4787–4795.
Klein, S.L., 1987. The first cleavage furrow demarcates the dorsal-ventral axis in Xenopus embryos. Dev. Biol. 120, 299–304.
Kono, Y., Horie, M., Takano, M., Otani, H., Xie, L.H., Akao, M., Tsuji, K., Sasayama, S., 2000. The properties of the Kir6.1–6.2 tandem channel co-expressed with SUR2A. Pflugers Arch 440, 692–698.
Koster, J.C., Marshall, B.A., Ensor, N., Corbett, J.A., Nichols, C.G., 2000. Targeted overactivity of beta cell K(ATP) channels induces profound neonatal diabetes. Cell 100, 645–654.
Kramer, K.L., Barnette, J.E., Yost, H.J., 2002. PKCgamma regulates syndecan-2 inside-out signaling during xenopus left–right development. Cell 111, 981–990.
Kreiling, J.A., Balantac, Z.L., Crawford, A.R., Ren, Y., Toure, J., Zchut, S., Kochilas, L., Creton, R., 2008. Suppression of the endoplasmic reticulum calcium pump during zebrafish gastrulation affects left–right asymmetry of the heart and brain. Mech. Dev. 125, 396–410.
Kubo, Y., Adelman, J.P., Clapham, D.E., Jan, L.Y., Karschin, A., Kurachi, Y., Lazdunski, M., Nichols, C.G., Seino, S., Vandenberg, C.A., 2005. International Union of

Pharmacology. LIV. Nomenclature and molecular relationships of inwardly rectifying potassium channels. Pharmacol Rev. 57, 509–526.
Kurpios, N.A., Ibanes, M., Davis, N.M., Lui, W., Katz, T., Martin, J.F., Belmonte, J.C., Tabin, C.J., 2008. The direction of gut looping is established by changes in the extracellular matrix and in cell:cell adhesion. Proc. Natl Acad. Sci. USA 105, 8499–8506.
Lalli, M.J., Johns, D.C., Janecki, M., Liu, Y., O'Rourke, B., Marban, E., 1998. Suppression of KATP currents by gene transfer of a dominant negative Kir6.2 construct. Pflugers Arch 436, 957–961.
Lang, F., Vallon, V., Knipper, M., Wangemann, P., 2007. Functional significance of channels and transporters expressed in the inner ear and kidney. Am. J. Physiol. Cell Physiol. 293, C1187–C1208.
Levin, M., 1998. Left–right asymmetry and the chick embryo. Semin. Cell Dev. Biol. 9, 67–76.
Levin, M., 2006. Is the early left–right axis like a plant, a kidney, or a neuron? The integration of physiological signals in embryonic asymmetry. Birth Defects Res. C Embryo Today 78, 191–223.
Levin, M., Buznikov, G.A., Lauder, J.M., 2006. Of minds and embryos: left–right asymmetry and the serotonergic controls of pre-neural morphogenesis. Dev. Neurosci. 28, 171–185.
Levin, M., Johnson, R.L., Stern, C.D., Kuehn, M., Tabin, C., 1995. A molecular pathway determining left–right asymmetry in chick embryogenesis. Cell 82, 803–814.
Levin, M., Mercola, M., 1998a. Gap junctions are involved in the early generation of left right asymmetry. Dev. Biol. 203, 90–105.
Levin, M., Mercola, M., 1998b. Gap junctions are involved in the early generation of left–right asymmetry. Dev. Biol. 203, 90–105.
Levin, M., Mercola, M., 1999. Gap junction-mediated transfer of left–right patterning signals in the early chick blastoderm is upstream of Shh asymmetry in the node. Development 126, 4703–4714.
Levin, M., Nascone, N., 1997. Two molecular models of initial left–right asymmetry generation. Med. Hypotheses 49, 429–435.
Levin, M., Pagan, S., Roberts, D.J., Cooke, J., Kuehn, M.R., Tabin, C.J., 1997. Left/right patterning signals and the independent regulation of different aspects of Situs in the chick embryo. Dev. Biol. 189, 57–67.
Levin, M., Palmer, A.R., 2007. Left–right patterning from the inside out: widespread evidence for intracellular control. Bioessays. 29, 271–287.
Levin, M., Thorlin, T., Robinson, K.R., Nogi, T., Mercola, M., 2002. Asymmetries in H+/K+-ATPase and cell membrane potentials comprise a very early step in left–right patterning. Cell 111, 77–89.
Light, P.E., Kanji, H.D., Fox, J.E., French, R.J., 2001. Distinct myoprotective roles of cardiac sarcolemmal and mitochondrial KATP channels during metabolic inhibition and recovery. FASEB J. 15, 2586–2594.
Lockwood, C., Zaidel-Bar, R., Hardin, J., 2008. The C. elegans zonula occludens ortholog cooperates with the cadherin complex to recruit actin during morphogenesis. Curr. Biol. 18, 1333–1337.
Lohr, J.L., Danos, M.C., Yost, H.J., 1997. Left-right asymmetry of a nodal-related gene is regulated by dorsoanterior midline structures during Xenopus development. Dev. Suppl. 124, 1465–1472.
Lu, C., Halvorsen, S., 1997. Channel activators regulate ATP-sensitive potassium channel (Kir6.1) expression in chick cardiomyocytes. FEBS Lett. 412, 121–125.
Maisonneuve, C., Guilleret, I., Vick, P., Weber, T., Andre, P., Beyer, T., Blum, M., Constam, D.B., 2009. Bicaudal C, a novel regulator of Dvl signaling abutting RNA-processing bodies, controls cilia orientation and leftward flow. Development 136, 3019–3030.
Malhotra, J.D., Kazen-Gillespie, K., Hortsch, M., Isom, L.L., 2000. Sodium channel beta subunits mediate homophilic cell adhesion and recruit ankyrin to points of cell–cell contact. J. Biol. Chem. 275, 11383–11388.
Marcus, D.C., Wu, T., Wangemann, P., Kofuji, P., 2002. KCNJ10 (Kir4.1) potassium channel knockout abolishes endocochlear potential. Am. J. Physiol. Cell Physiol. 282, C403–C407.
Marshall, L.J., Muimo, R., Riemen, C.E., Mehta, A., 1999. Na+ and K+ regulate the phosphorylation state of nucleoside diphosphate kinase in human airway epithelium. Am. J. Physiol. 276, C109–C119.
Masho, R., 1990. Close correlation between the 1st cleavage plane and the body axis in early Xenopus embryos. Dev. Growth Differ. 32, 57–64.
Masia, R., De Leon, D.D., MacMullen, C., McKnight, H., Stanley, C.A., Nichols, C.G., 2007. A mutation in the TMD0-L0 region of sulfonylurea receptor-1 (L225P) causes permanent neonatal diabetes mellitus (PNDM). Diabetes 56, 1357–1362.
Matter, K., Balda, M.S., 2003. Signalling to and from tight junctions. Nat. Rev. Mol. Cell Biol. 4, 225–236.
McEwen, D.P., Isom, L.L., 2004. Heterophilic interactions of sodium channel beta1 subunits with axonal and glial cell adhesion molecules. J. Biol. Chem. 279, 52744–52752.
McGrath, J., Somlo, S., Makova, S., Tian, X., Brueckner, M., 2003. Two populations of node monocilia initiate left–right asymmetry in the mouse. Cell 114, 61–73.
Merzdorf, C.S., Chen, Y.H., Goodenough, D.A., 1998. Formation of functional tight junctions in Xenopus embryos. Dev. Biol. 195, 187–203.
Miki, T., Seino, S., 2005. Roles of KATP channels as metabolic sensors in acute metabolic changes. J. Mol. Cell. Cardiol. 38, 917–925.
Morokuma, J., Blackiston, D., Levin, M., 2008. KCNQ1 and KCNE1 K+ channel components are involved in early left–right patterning in Xenopus laevis embryos. Cell. Physiol. Biochem. 21, 357–372.
Newport, J., Kirschner, M., 1982a. A major developmental transition in early Xenopus embryos: I. Characterization and timing of cellular changes at the midblastula stage. Cell 30, 675–686.
Newport, J., Kirschner, M., 1982b. A major developmental transition in early Xenopus embryos: II. Control of the onset of transcription. Cell 30, 687–696.
Nichols, C.G., 2006. KATP channels as molecular sensors of cellular metabolism. Nature 440, 470–476.
Nieto, M.A., Patel, K., Wilkinson, D.G., 1996. In situ hybridization analysis of chick embryos in whole mount and tissue sections. Methods Cell Biol. 51, 219–235.
Nieuwkoop, P.D., Faber, J., 1967. Normal Table of *Xenopus laevis* (Daudin). North-Holland Publishing Company, Amsterdam.
Noma, A., 1983. ATP-regulated K+ channels in cardiac muscle. Nature 305, 147–148.
Pagan-Westphal, S., Tabin, C., 1998. The transfer of left–right positional information during chick embryogenesis. Cell 93, 25–35.
Peeters, H., Devriendt, K., 2006. Human laterality disorders. Eur. J. Med. Genet. 49, 349–362.
Pennekamp, P., Karcher, C., Fischer, A., Schweickert, A., Skryabin, B., Horst, J., Blum, M., Dworniczak, B., 2002. The ion channel polycystin-2 is required for left–right axis determination in mice. Curr. Biol. 12, 938–943.
Pountney, D.J., Sun, Z.Q., Porter, L.M., Nitabach, M.N., Nakamura, T.Y., Holmes, D., Rosner, E., Kaneko, M., Manaris, T., Holmes, T.C., Coetzee, W.A., 2001. Is the molecular composition of K(ATP) channels more complex than originally thought? J. Mol. Cell. Cardiol. 33, 1541–1546.
Pu, J.L., Ye, B., Kroboth, S.L., McNally, E.M., Makielski, J.C., Shi, N.Q., 2008. Cardiac sulfonylurea receptor short form-based channels confer a glibenclamide-insensitive KATP activity. J. Mol. Cell. Cardiol. 44, 188–200.
Qiu, D., Cheng, S.M., Wozniak, L., McSweeney, M., Perrone, E., Levin, M., 2005. Localization and loss-of-function implicates ciliary proteins in early, cytoplasmic roles in left–right asymmetry. Dev. Dyn. 234, 176–189.
Rajasekaran, S.A., Beyenbach, K.W., Rajasekaran, A.K., 2008. Interactions of tight junctions with membrane channels and transporters. Biochim. Biophys. Acta 1778, 757–769.
Ramsdell, A.F., 2005. Left–right asymmetry and congenital cardiac defects: getting to the heart of the matter in vertebrate left–right axis determination. Dev. Biol. 288, 1–20.
Raya, A., Kawakami, Y., Rodriguez-Esteban, C., Ibanes, M., Rasskin-Gutman, D., Rodriguez-Leon, J., Buscher, D., Feijo, J.A., Izpisua Belmonte, J.C., 2004. Notch activity acts as a sensor for extracellular calcium during vertebrate left–right determination. Nature 427, 121–128.
Reimann, F., Ashcroft, F.M., 1999. Inwardly rectifying potassium channels. Curr. Opin. Cell Biol. 11, 503–508.
Sampath, K., Cheng, A.M., Frisch, A., Wright, C.V., 1997. Functional differences among Xenopus nodal-related genes in left–right axis determination. Development 124, 3293–3302 Supplement.
Sanders, E.J., Dicaprio, R.A., 1976. Intercellular junctions in the Xenopus embryo prior to gastrulation. J. Exp. Zool. 197, 415–421.
Sarmah, B., Latimer, A.J., Appel, B., Wente, S.R., 2005. Inositol polyphosphates regulate zebrafish left–right asymmetry. Dev. Cell 9, 133–145.
Schneider, I., Houston, D.W., Rebagliati, M.R., Slusarski, D.C., 2007. Calcium fluxes in dorsal forerunner cells antagonize {beta}-catenin and alter left–right patterning. Development.
Schwappach, B., Zerangue, N., Jan, Y.N., Jan, L.Y., 2000. Molecular basis for K(ATP) assembly: transmembrane interactions mediate association of a K+ channel with an ABC transporter. Neuron 26, 155–167.
Schweickert, A., Weber, T., Beyer, T., Vick, P., Bogusch, S., Feistel, K., Blum, M., 2007. Cilia-driven leftward flow determines laterality in Xenopus. Curr. Biol. 17, 60–66.
Seharaseyon, J., Sasaki, N., Ohler, A., Sato, T., Fraser, H., Johns, D.C., O'Rourke, B., Marban, E., 2000. Evidence against functional heteromultimerization of the KATP channel subunits Kir6.1 and Kir6.2. J. Biol. Chem. 275, 17561–17565.
Shibata, T., Hibino, H., Doi, K., Suzuki, T., Hisa, Y., Kurachi, Y., 2006. Gastric type H+, K+-ATPase in the cochlear lateral wall is critically involved in formation of the endocochlear potential. Am. J. Physiol. Cell Physiol. 291, C1038–C1048.
Shimeld, S.M., Levin, M., 2006. Evidence for the regulation of left–right asymmetry in Ciona intestinalis by ion flux. Dev. Dyn. 235, 1543–1553.
Shimomura, K., 2009. The K(ATP) channel and neonatal diabetes. Endocr. J. 56, 165–175.
Simard, A., Di Pietro, E., Young, C.R., Plaza, S., Ryan, A.K., 2006. Alterations in heart looping induced by overexpression of the tight junction protein Claudin-1 are dependent on its C-terminal cytoplasmic tail. Mech. Dev. 123, 210–227.
Sivaprasadarao, A., Taneja, T.K., Mankouri, J., Smith, A.J., 2007. Trafficking of ATP-sensitive potassium channels in health and disease. Biochem. Soc. Trans. 35, 1055–1059.
Sive, H.L., Grainger, R.M., Harland, R.M., 2000. Early Development of Xenopus Laevis. Cold Spring Harbor Laboratory Press, New York.
Slesinger, P.A., Patil, N., Liao, Y.J., Jan, Y.N., Jan, L.Y., Cox, D.R., 1996. Functional effects of the mouse weaver mutation on G protein-gated inwardly rectifying K+ channels. Neuron 16, 321–331.
Speder, P., Petzoldt, A., Suzanne, M., Noselli, S., 2007. Strategies to establish left/right asymmetry in vertebrates and invertebrates. Curr. Opin. Genet. Dev.
Spruce, A.E., Standen, N.B., Stanfield, P.R., 1985. Voltage-dependent ATP-sensitive potassium channels of skeletal muscle membrane. Nature 316, 736–738.
Standen, N.B., Quayle, J.M., Davies, N.W., Brayden, J.E., Huang, Y., Nelson, M.T., 1989. Hyperpolarizing vasodilators activate ATP-sensitive K+ channels in arterial smooth muscle. Science 245, 177–180.
Suzuki, M., Kotake, K., Fujikura, K., Inagaki, N., Suzuki, T., Gonoi, T., Seino, S., Takata, K., 1997. Kir6.1: a possible subunit of ATP-sensitive K+ channels in mitochondria. Biochem. Biophys. Res. Commun. 241, 693–697.
Suzuki, M., Saito, T., Sato, T., Tamagawa, M., Miki, T., Seino, S., Nakaya, H., 2003. Cardioprotective effect of diazoxide is mediated by activation of sarcolemmal but not mitochondrial ATP-sensitive potassium channels in mice. Circulation 107, 682–685.
Tabin, C., 2005. Do we know anything about how left–right asymmetry is first established in the vertebrate embryo? J. Mol. Histol. 1–7.

Tabin, C.J., Vogan, K.J., 2003. A two-cilia model for vertebrate left–right axis specification. Genes Dev. 17, 1–6.
Tinker, A., Jan, Y.N., Jan, L.Y., 1996. Regions responsible for the assembly of inwardly rectifying potassium channels. Cell 87, 857–868.
Toyoizumi, R., Kobayashi, T., Kikukawa, A., Oba, J., Takeuchi, S., 1997. Adrenergic neurotransmitters and calcium ionophore-induced situs inversus viscerum in Xenopus laevis embryos. Dev. Growth Differ. 39, 505–514.
Toyoizumi, R., Ogasawara, T., Takeuchi, S., Mogi, K., 2005. Xenopus nodal related-1 is indispensable only for left–right axis determination. Int. J. Dev. Biol. 49, 923–938.
van Bever, L., Poitry, S., Faure, C., Norman, R.I., Roatti, A., Baertschi, A.J., 2004. Pore loop-mutated rat KIR6.1 and KIR6.2 suppress KATP current in rat cardiomyocytes. Am. J. Physiol. Heart Circ. Physiol. 287, H850–H859.
Van Itallie, C.M., Fanning, A.S., Bridges, A., Anderson, J.M., 2009. ZO-1 stabilizes the tight junction solute barrier through coupling to the perijunctional cytoskeleton. Mol. Biol. Cell 20, 3930–3940.
Van Laer, L., Carlsson, P.I., Ottschytsch, N., Bondeson, M.L., Konings, A., Vandevelde, A., Dieltjens, N., Fransen, E., Snyders, D., Borg, E., Raes, A., Van Camp, G., 2006. The contribution of genes involved in potassium-recycling in the inner ear to noise-induced hearing loss. Hum. Mutat. 27, 786–795.
Vandenberg, L.N., Levin, M., 2009. Perspectives and open problems in the early phases of left–right patterning. Semin. Cell Dev. Biol. 20, 456–463.
Vanhoven, M.K., Bauer Huang, S.L., Albin, S.D., Bargmann, C.I., 2006. The claudin superfamily protein nsy-4 biases lateral signaling to generate left–right asymmetry in C. elegans olfactory neurons. Neuron 51, 291–302.
Vize, P.D., Melton, D.A., Hemmati-Brivanlou, A., Harland, R.M., 1991. Assays for gene function in developing Xenopus embryos. Meth. Cell Biol. 36, 367–387.
Warner, A.E., Guthrie, S.C., Gilula, N.B., 1984. Antibodies to gap-junctional protein selectively disrupt junctional communication in the early amphibian embryo. Nature 311, 127–131.
Whitman, M., Mercola, M., 2001a. TGF-beta superfamily signaling and left–right asymmetry. Sci. STKE 2001, RE1.
Whitman, M., Mercola, M., 2001b. TGF-beta superfamily signaling and left–right asymmetry. Science's STKE [Electronic Resource]: Signal Transduction Knowledge Environment. 2001, RE1.
Xu, J., Van Keymeulen, A., Wakida, N.M., Carlton, P., Berns, M.W., Bourne, H.R., 2007. Polarity reveals intrinsic cell chirality. Proc. Natl Acad. Sci. USA 104, 9296–9300.
Yamauchi, H., Miyakawa, N., Miyake, A., Itoh, N., 2009. Fgf4 is required for left–right patterning of visceral organs in zebrafish. Dev. Biol. 332, 177–185.
Yost, H.J., 1999. Diverse initiation in a conserved left–right pathway? Curr. Opin. Genet. Dev. 9, 422–426.
Yost, H.J., 2001. Establishment of left–right asymmetry. Int. Rev. Cytol. 203, 357–381.
Zerangue, N., Schwappach, B., Jan, Y.N., Jan, L.Y., 1999. A new ER trafficking signal regulates the subunit stoichiometry of plasma membrane K(ATP) channels. Neuron 22, 537–548.
Zobel, C., Cho, H.C., Nguyen, T.T., Pekhletski, R., Diaz, R.J., Wilson, G.J., Backx, P.H., 2003. Molecular dissection of the inward rectifier potassium current (IK1) in rabbit cardiomyocytes: evidence for heteromeric co-assembly of Kir2.1 and Kir2.2. J. Physiol. 550, 365–372.